TECHNICAL UNIVERSITY OF LIBEREC
Faculty of Mechanical Engineering

Influence of the Zinc Coated Sheets Surface Treatment on the Friction Coefficient

Master thesis

Study programme: N2301 – Mechanical Engineering
Study branch: 2301T048 – Engineering Technology and Materiales

Author: **Shailender Ezhilarasan**
Supervisor: Ing. Jiří Sobotka, Ph.D.

Liberec 2018

Technical University of Liberec
Faculty of Mechanical Engineering
Academic year: **2017/2018**

DIPLOMA THESIS ASSIGNMENT

(PROJECT, ART WORK, ART PERFORMANCE)

First name and surname:	**Shailender Ezhilarasan**
Study program:	**N2301 Mechanical Engineering**
Identification number:	**S16000541**
Specialization:	**Engineering Technology and Materiales**
Topic name:	**Influence of the Zinc Coated Sheets Surface Treatment on the Friction Coefficient**
Assigning department:	**Department of Engineering Technology**

Rules for elaboration:

1. Basic types of protective coatings for sheets designed for drawing stampings.
2. Tribology in the metal forming processes.Importance of friction at metal forming. Overview of tests used for evaluation tribological properties of sheets.
3. Experimental determination of the surface treatment influence on the friction coefficient in dependence on the technological parameters (feed rate, magnitude of contact pressure) by the strip drawing test.
4. Evaluation of the experiment. Creation of 3D surface color maps.
5. Conclusion and recommendations for further research.

Scope of graphic works: **tables, graphs**

Scope of work report
(scope of dissertation): **approx. 50 p**

Form of dissertation elaboration: **printed/electronical**

List of specialized literature:

[1] TOTTEN, G.E. ed. *Handbook of Lubrication and Tribology: Volume I - Application and Maintenance.* **2nd ed. Boca Raton: CRC Press, 2006, p. 1159. ISBN 978-0-8493-2095-8.**
[2] STACHOWIAK, G.W., BATCHELOR, A.W. *Engineering tribology.* **4thed. Oxford: Butterworth-Heinemann, 2014. p. 884. ISBN 978-0-123-9-70473.**
[3] MANG, T., DRESEL, W. *Lubricants and Lubrication.***2nd ed. Weinheim: WILEY-VCH Verlag, 2007. p. 894. ISBN: 978-3-527-31497-3.**
[4] TRACTON, A.A. *Coating materials and surface coatings.* **London:Taylor & Francis Group, 2007. 464 s.ISBN 1-4200-4404-4**
[5] DAVIES, G. *Materials for Automobile Bodies.* **Oxford: Butterworth-Heinemann, 2003. p. 277. ISBN 0-7506-5692-1.**

Tutor for dissertation: **Ing. Jiří Sobotka, Ph.D.**
Department of Engineering Technology

Dissertation Counsellor: **doc. Ing. Pavel Solfronk, Ph.D.**
Department of Engineering Technology

Date of dissertation assignment: **31 October 2017**

Date of dissertation submission: **31 January 2019**

prof. Dr. Ing. Petr Lenfeld
Dean

L.S.

doc. Ing. Jaromír Moravec, Ph.D.
Head of Department

Liberec, dated: 1 November 2017

Declaration:

I hereby certify that I have been informed the Act 121/2000, the Copyright Act of the Czech Republic, namely § 60 – Schoolwork, applies to my master thesis in full scope.

I acknowledge that the Technical University of Liberec (TUL) does not infringe my copyrights by using my master thesis for TUL's internal purposes.

I am aware of my obligation to inform TUL on having used or licensed to use my master thesis; in such a case TUL may require compensation of costs spent on creating the work at up to their actual amount.

I have written my master thesis myself using literature listed therein and consulting it with my thesis supervisor and my tutor.

Concurrently, I confirm that the printed version of my master thesis is coincident with an electronic version, inserted into IS STAG.

Date:

Signature:

Annotation:

The main aim of this thesis was to carry out tribological measurement and comparison of tribological results for two selected surface treatments. That is why this thesis deals with the tribological testing and comparison of results for zinc coated sheets. Two different types of surface coatings (hot dip galvanized – HDG and new inorganic treatment – NIT) on deep drawing steel sheet were tested by a tribological test called as strip drawing test on the testing device SOKOL400 under the combinations of feed rates v [mm/sec] and contact pressure p [MPa]. Firstly, different kinds of forces (F_{max}, F_h, F_{avg}, F_{min} and ΔF) were evaluated for both tested surfaces. Moreover, the friction coefficient μ [1] was computed as well. For better overview of final results, there were finally created 3D color map surface graphs. According to the results, NIT coating revealed a much better tribological behavior than HDG coating under the higher feed rates and especially under the higher contact pressures. However, these data are needed to be verified by more experiments and other kind of testing (with different coatings) is also necessary to be performed.

Keywords:

Tribology, Surface Treatment, Friction Coefficient, Strip Drawing Test, 3D Color Map Surface Graph

This diploma thesis was written at the Technical University of Liberec as part of the Student Grant Contest "SGS 21122" with the support of the Specific University Research Grant, as provided by the Ministry of Education, Youth and Sports of the Czech Republic in the year 2018.

Acknowledgement:

At this pleasing movement of having successfully completed my thesis, I would like to convey my sincere thanks and gratitude to my supervisor Ing. Jiri Sobotka PhD. Thank you for being such a supportive tutor. You have educated me countless lessons academically as well as during my thesis work. I really value you in so many ways because without having you my dear tutor, I would not have finished my thesis successfully. You are such an inspiration to me. You're teachings are motivating and indeed very applicable in my future career. Thank you for being so dedicated towards this cause.

I would like to thank the Department of Technology and Materials, Technical University of Liberec throughout my masters course.

Finally I would like to thank god and my family members for giving me this priceless opportunity and never ending support.

TABLE OF CONTENTS

List of Used Symbols and Units

F_T	-	Drawing force	[N]
F_N	-	Normal force	[N]
μ	-	Friction coefficient	[1]
μ_o	-	Static friction	[1]
μ_k	-	Kinetic friction	[1]
η	-	dynamic viscosity of the lubricant	[Pa·sec]
N	-	Rotation speed	[rpm]
p_{av}	-	Average bearing pressure	[MPa]
h	-	film thickness	[mm]
λ	-	lambda	[1]
S	-	Contact area	[mm^2]
p	-	Contact pressure	[MPa]
F_o	-	Bending force on the drawing edge	[N]
$F_{T1,2,3}$	-	Drawing forces for different tribological tests	[N]
α	-	Angle of contact	[1]
μ_2	-	Friction coefficient on the drawing edge	[1]
σ_y	-	Yield strength	[MPa]
σ_m	-	Ultimate strength	[MPa]
A_{80mm}	-	Total ductility	[%]
E	-	Young's modulus	[GPa]
ρ	-	Density	[$g.cm^{-3}$]
v	-	Feed rate	[mm/sec]
R_a	-	Roughness average	[µm]
R_{Pc}	-	Peak count	[1/cm]
F_{max}	-	Maximal force	[N]
F_h	-	Maximal force in stable zone	[N]
F_{min}	-	Minimal force in stable zone	[N]
F_{avg}	-	Average force in stable zone	[N]
ΔF	-	Peak to valley force (F_h-F_{min})	[N]

1. INTRODUCTION

This thesis is mainly focused on calculating friction coefficient μ [1] magnitude of the zinc coated sheets. Friction plays an important role in daily life (see Fig. 1.1) and extensive researches are being carried out to reduce friction and its effects, but it can't be avoided completely. It can be reduced to a certain extent by using e.g. some effective coatings on the surface of the material through various techniques like physical vapour deposition (PVD), chemical vapour deposition (CVD), hot dip galvanizing (HDG), etc. These coatings help to reduce the friction and wear as well.

The present work is focused on performing tribological tests of zinc coated sheets in the form of strips. Such strip of sheet was subjected to different tribological conditions and on the basis of Coloumb's law, the applied drawing force F_T [N] and normal force F_N [N] were measured and friction coefficient μ [1] could be found.

The main objective of this thesis was to examine a trial strip of sheet with different coatings (HDG and NIT) under the different basic tribological parameters – namely feed rate v [mm/min] and contact pressure p [MPa]. Their final comparison was done by 3D color map surfaces graphs. The final analysis (forces) of the surface coatings characteristics and the characteristics of film failure (galling) due to friction and wear helped to describe the results. Although the complete efficiency cannot be obtained here, some improvements and developments can be seen.

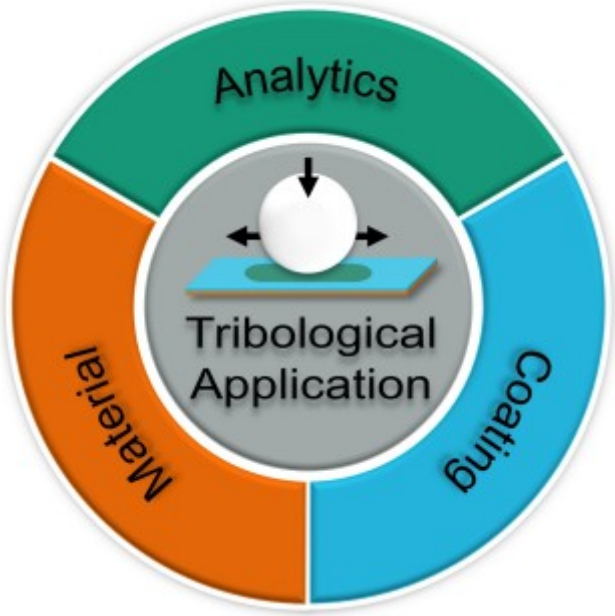

Fig. 1.1 *Lubricating for Friction [1]*

2. TRIBOLOGY

Tribology is quite very new field of science, most knowledge has been gained after the second world war. Tribology is still in imperfect state and subject to some controversy which has impeded the diffusion. Tribology is focused on friction, wear and lubrication of interacting surfaces in relative motion. Friction between interacting surface is the cause for wear and it's the major cause for wastage of material. In every invention of mankind there is wear from household to aircrafts. Tribology gives the analysis solution to overcome this wear by lubrication. Even our human body has some parts like bone joints which get into wear and are lubricated naturally [2]. The two major divisions of tribology are:

- the characteristics of films between the contacting surfaces,
- the characteristics of film failure due to severe friction and wear.

2.1. Tribology in Light of History

Tribology is derived from the Greek word "Tribos" which means rubbing or sliding. The scientific study of tribology also has a long history and many of the basic laws of friction (such as the proportionality between normal force and limiting friction force) are thought to have been developed by Leonardo da Vinci in the late 15th century. In Fig. 2.1 is shown tribology during early civilizations. [2]

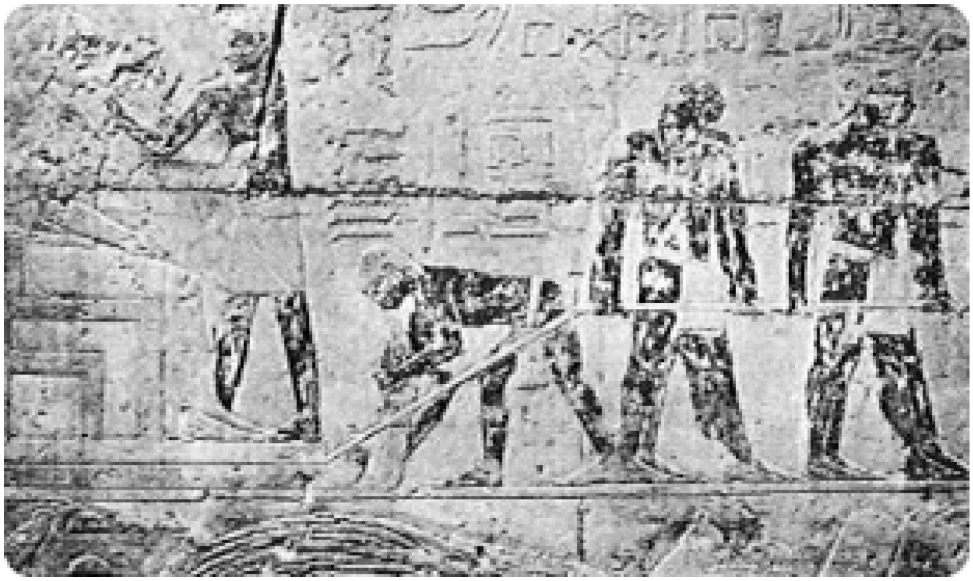

Fig. 2.1 *Tribology during early civilization [3]*

Leonardo da Vinci (1452-1519) can be called as father of modern tribology (see Fig. 2.2). He explained tribological topics like friction, wear, bearing materials, plain bearings, lubrication systems, gears, screw jacks and rolling element bearings. [4] After that, it was proposed by Amonton in 1699 that surfaces are covered by small spheres and that the friction coefficient is a result of the contact angle between contacting surface spheres. He assumed that motion was always on the top of the spheres. Nevertheless, no one bothered about the motion of the spheres in downward direction. In 1886 Osborne Reynolds published a paper on hydrodynamic lubrication. According to Reynolds, hydrodynamic pressure liquid entrained between sliding surfaces was sufficient to prevent contact between surfaces at low sliding speeds. This experiment has found good practical application in railway axle bearing, which gave lower friction. But after the invention of scanning electron microscope (SEM), it is possible to learn its nature deeply.

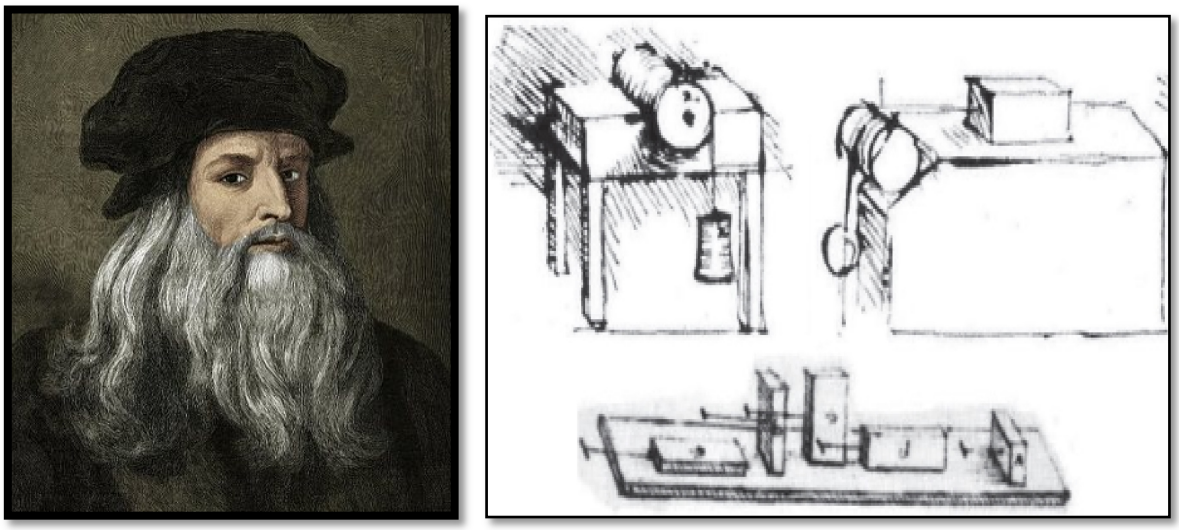

Fig. 2.2 *Tribology according to Leonardo da Vinci [5, 6]*

2.2. Friction

Friction is the resistance to relation motion of contacting bodies. Friction is of many types that include dry, lubricating, sliding, rolling, dynamic, kinetic, static (starting or limiting), internal (hysteretic), external and viscous. In the above friction types, some of them are considered as more important - like static friction and dynamic friction. Generally speaking, friction has caused failures. But it's useful in some instances like without friction human can't walk, cars can't move etc. [2]

STATIC FRICTION- it is the friction between two surfaces that are not in relative motion. For example, consider a car that is about to start, there is static friction between tire and road, which prevents slipping of the tire from the road.

DYNAMIC FRICTION- it is the friction between two surfaces that are in relative motion to each other. For example, the same car has started moving and the dynamic friction between the road and tire prevents slipping against the road. [8]

2.2.1. Basic Laws of Friction

All basic laws of friction aroused from the simple model – block on table. These model laws help in finding the direction and magnitude of the friction force between two bodies with dry surfaces in contact.

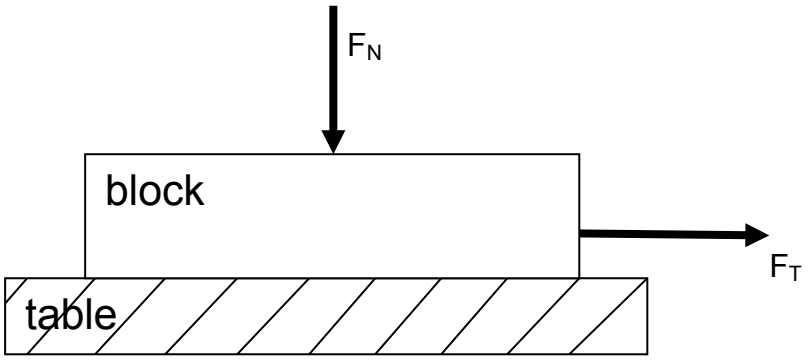

Fig. 2.3 *Friction according to Amontons*

In the Fig. 2.3, drawing force F_T is needed to make the block slide on table to keep it moving constant. The drawing force F_T depends on the value of normal force F_N. Amontons law can be understood by the relation between drawing force F_T and the normal force F_N as following:

$$F_T = \mu F_N \tag{1}$$

Where,

μ	-	friction coefficient	[1]
F_N	-	normal force	[N]
F_T	-	drawing force	[N]

The friction coefficient depends on the material. During the static condition it is called as the static friction (μ_0) and during kinetic condition it is kinetic friction (μ_k).

AMONTON'S LAWS OF FRICTION

Leonardo da Vinci observed the same relations 200 years earlier. But these results were not known to scientific world of Amontons time. Amontons found that friction was caused by the interaction of surface roughness peaks and he found that asperities slide up and down for more elastic materials. He also suggested that sliding would push aside the surface irregularity peaks. According to Amontons, the laws can be described as following:

- the force of friction is directly proportional to the applied load,
- the force of friction is independent of the apparent area of contact.

However, for better understanding, the friction laws of Amontons can be described in four steps as listed below: [2, 4]

- the resistance caused by friction increases or decreases in proportion to the pressure,
- the resistance caused by friction is the same for iron, copper, lead and wood as long as they are lubricated with lubricants,
- the resistance is roughly equal to one-third of pressure,
- this resistance does not depend on velocity and other conditions.

COULOMB'S LAW OF FRICTION

Charles-Augustin de Coulomb (1736 -1806) was a French physicist and also engineer. He found that mechanical interlocking of asperities is the cause for friction and the actual surface material on the individual asperities was functionless. According to him "Friction and cohesion are not active forces like gravity, which always exerts its full effect, but only passive forces; these two forces can be measured by the limits of their strength". Although his explanation was wrong, his law is still used for dry friction under the condition where heavy plastic deformation occurs. According to Coulomb, the law can be described as:

- kinetic friction is independent of the sliding velocity.

However, on the debate of Coulomb and Amontons, Coulomb found the independence of the coefficient of friction on velocity, normal force, contact area and roughness are only a first very rough approximation. He also differentiated between material couples e.g., metal-metal. In all cases the dependencies. To solve this, the geometric and loading parameters have to be changed by several orders of magnitude to achieve a change in the friction coefficient by two. [2, 4]

2.2.2. Classification of Frictional Contacts

The main reason for friction in mechanical component is sliding. There are four categories of friction with high and low frictional force which are given below.

I. FORCE TRANSMITTING COMPONENTS

Force transmitting components operate without displacement. There are two classes of surfaces – drive and clamped surfaces.

DRIVE SURFACES - there is no macroscopic slip on these surfaces. Static friction is higher than dynamic friction in these surfaces. As some of the examples there are power belts, shoes on the floor, tires and wheels.

CLAMPED SURFACES - in clamped surfaces, a friction force frequently produces a microscopic slip. So, the system must be designed to impose high normal (clamping) force. Since contact pressures may vary, local sliding may occur when low value of friction force is applied. As some examples of clamped surfaces there are press fitted pulleys on shafts, or bolted joining surfaces in machines and so on. [7]

II. ENERGY ABSORPTION CONTROLLING COMPONENTS

Mostly these components are seen in braking and clutching systems. An important requirement in these components is constant friction which will prevent sudden failures. Another important factor is to minimize the difference between static and dynamic friction coefficient to avoid vibration in such components. As good examples there are brakes and clutches (see Fig. 2.5). [8]

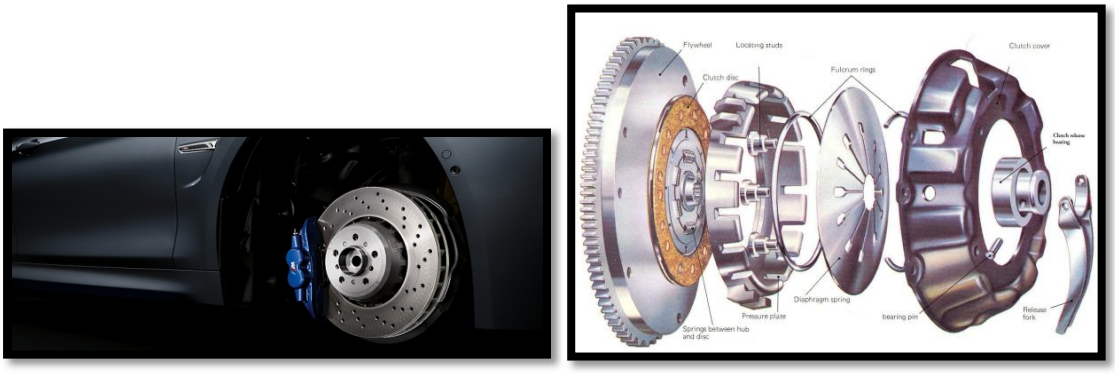

Fig. 2.5 *Brakes and clutches [9,10]*

III. QUALITY CONTROL COMPONENTS

In these components, a constant friction is required. If the friction is above or below the required constant level, the required properties cannot be achieved. There are two examples:

a) in knitting and weaving the tightness of weave must be controlled to produce uniform fabric,
b) in sheet metal rolling mills, constant friction coefficient is required to maintain uniform thickness and surface finish of the sheet.

IV. LOW FRICTION COMPONENTS

These are components that operate with maximum efficiency when a normal force is transmitted. As some examples there are gears in watches and bearings in motors. In these machines, high friction may produce distortion. [11]

2.2.3. Cost of Friction and Wear

When reviewed on a single machine, the cost of wear is very low. However, for a large number of machines, the cost of wear is very high. So the cost or benefit equation can be summarized as:

$$\left.\begin{array}{c}\textit{Total tribological costs}\\ \textit{or savings}\end{array}\right\} = \left\{\begin{array}{c}\textit{Sum of individual machine costs or}\\ \textit{savings} \times \textit{number of machines}\end{array}\right.$$

2.3. Surfaces

All surfaces are rough and its magnitude (roughness) depends on the surface treatment by various processes - e.g. casting or moulding (see Fig. 2.6). While seeing the polished surface through a electro-micrograph, it shows that they are covered with peaks and valleys. It means when two surfaces are placed together, the two peaks of the both surfaces touch and remaining area stand apart. That´s why where the peaks are flatter, the contact area increases and pressure decreases. [12]

Fig. 2.6 *Moulding [13]*

2.3.1. Measurement of Surface Roughness

As the main instruments there are profile analyzer and scanning election microscope (SEM). The SEM has many advantages, but are limited by specimen size and it cannot quantify roughness. Overview of these basic advantages and disadvantages is given in Tab. 2.1.

Tab. 2.1 *Advantages and disadvantages of SEM and profile analyzer*

	Advantages	**Disadvantages**
SEM	SEM can provide 3D and topographical image.	The specimen size is limited.
	It can provide micrographs with good resolution.	It cannot quantify roughness.
Profile Analyzer	It provides a sharp stylus and it detects the movement as it follows the texture.	Profiles should be positioned to avoid aberrations.
	Many flaws, inclusions, cracks could be identified.	

The surface profile contains three major components. [7]

ROUGHNESS-it is deviation from wavy surface, caused by cutting tool and it is caused by wear machining conditions, microstructure of the workpiece, vibrations in the system and so on. The height, width and closely spaced irregularities create predominant surface pattern.

WAVINESS- it is periodic deviations from the geometric surface, often sinusoidal in form and it is due to the low level oscillations of machine tool during machining. They are because of heat treatment of workpiece or machine deflections and vibrations.

ERROR OF FORM -they are not normally considered part of the surface texture. It is irregular surface deviation from the design profile and it is caused by lack of accuracy or stiffness of the machine system. [12]

2.3.2. Surface Roughness Parameters

Surface roughness refers to the variations in the height of the surface relative to a reference plane. It is measured along a set of parallel line profiles (2D measurement) and so-called surface maps (3D measurement).

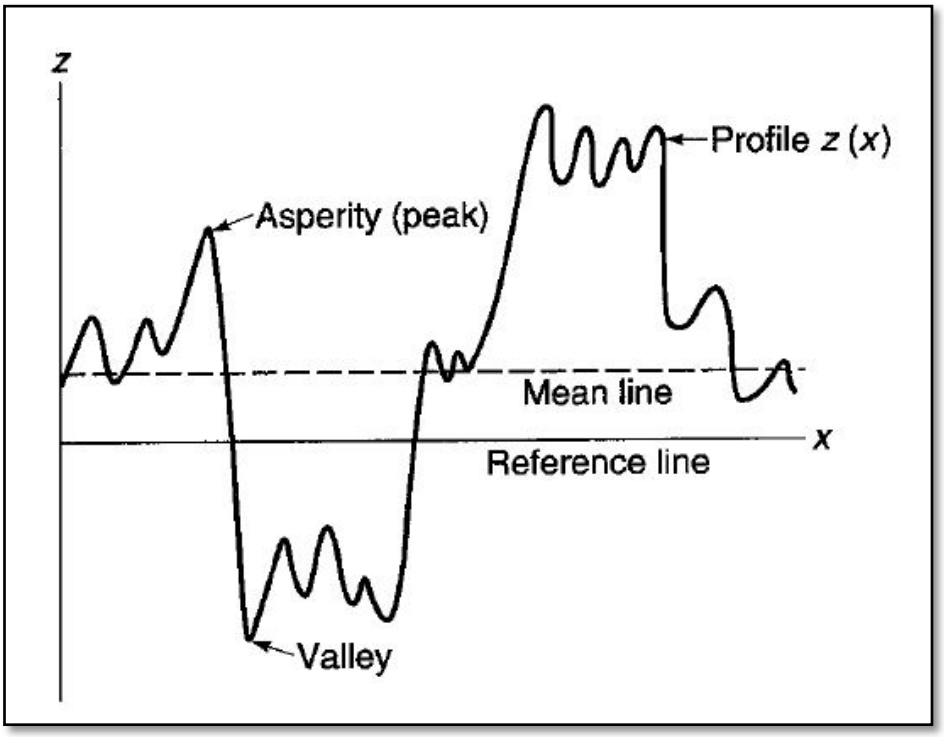

Fig. 2.7 *Schematic of the surface profile [7]*

To improve the performance of manufactured products, the surface texture of mechanical components has been checked for over 80 years. The first roughness tester recorded surface height using a stylus tip in contact with surface. The measured profile was written in a carbon sheet and recorded in a galvanometer. For a long time only R_a was the only known parameter and then came $R_{p,}$ $R_{pm.}$ Some of the surface roughness parameters are listed below:

R_a	-	Center line average or arithmetic average	[μm]
R_q	-	Root mean square	[μm]
R_p	-	Maximum peak height	[μm]
R_t	-	Maximum peak to valley height	[μm]
R_v	-	Maximum valley depth	[μm]
R_z	-	Average peak to valley height	[μm]
R_{pm}	-	Average peak to mean height	[μm]

2.4. Striebeck Curve

The three lubrication regimes named below are figured in the Striebeck curve. It explains the relation between friction coefficient and bearing parameter $\eta.N/p_{av}$, where η is dynamic viscosity of the lubricant [Pa·sec], N is rotation speed [rpm] and finally p_{av} is average bearing pressure [MPa].

These three regimes are explained by means of the Striebeck curve. The friction causes temperature increase and viscosity drops down. [12]

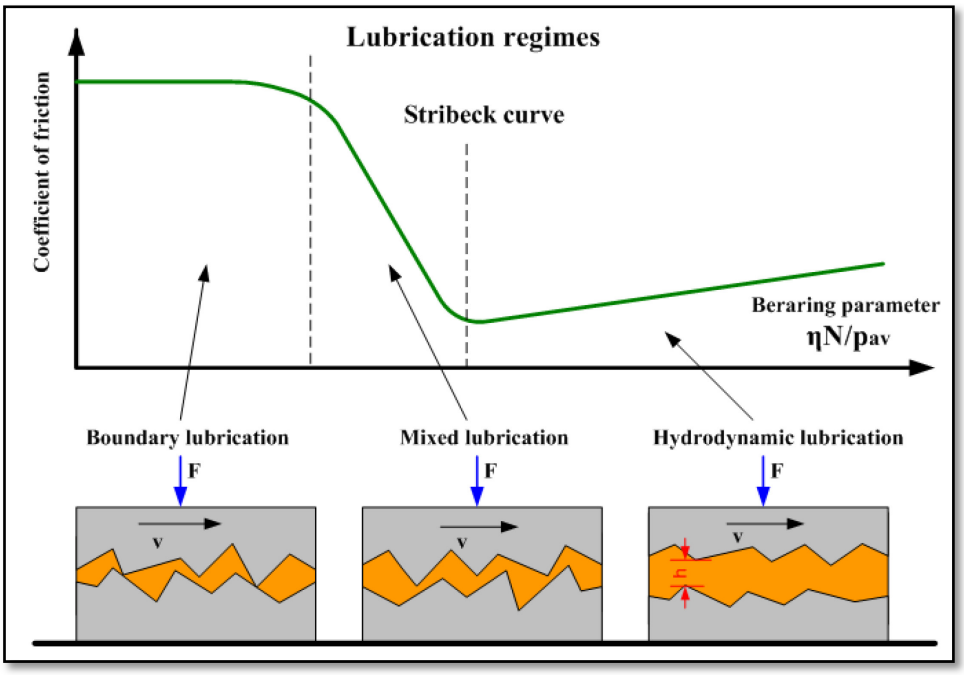

Fig. 2.8 *Striebeck curve lubrication regimes [14]*

2.4.1. Classification of Lubrication Regimes

Lubricants can be solid or liquid, but mostly it is focused on liquid lubricants under sliding conditions. It's difficult to form a smooth surface. When a smooth surface is examined under high magnification, it has some peaks and valleys (so called asperities). The lambda (λ) ratio is expressed by the equation below: [11]

$$\lambda = \frac{h}{R_a} \tag{3}$$

Where:

h	-	film thickness	[μm]
R_a	-	surface roughness	[μm]
λ	-	lambda	[1]

Lubricated friction is characterized by the presence of a thin film of pressurized lubricant (squeeze film) between the surface of the bearing and the journal. There are 4 types of lubrication regimes.

DRY LUBRICATION -it is the lubrication between two surfaces which reduce friction without liquid medium. This regime is very undesirable for metal forming.

BOUNDARY LUBRICATION -constant contact between friction surfaces at high surface points occur at boundary lubrication. Because of its high friction coefficient (energy loss), increased wear, possibility of seizure between the bearing and journal materials and non-uniform distribution of the bearing load (localized peaks) this regime is undesirable. Also very severe failures are caused by boundary lubrication.

MIXED LUBRICATION– it is intermediate regime between boundary and hydrodynamic lubrication. An intermittent contact between the friction surfaces at few high surface points (micro-asperities) occurs at mixed lubrication. In this regime due to temperature rise, the friction coefficient increases consequently. So mixed lubrication is unstable

HYDRODYNAMIC LUBRICATION– there is no contact between rubbing surfaces. High rotation speed at relatively low bearing loads results in hydrodynamic friction, which is characterized by stable squeeze film (oil film) between the rubbing surfaces. The squeeze film keeps the surface of the bearing and the shaft apart due to the force called hydrodynamic lift (see Fig. 2.9) generated by the lubricant squeezed through the convergent gap between the eccentric journal and bearing. In this regime due to rise in temperature, lower the viscosity causes friction coefficient to drop with consequent decrease of temperature. So finally stated, hydrodynamic lubrication is stable. [15]

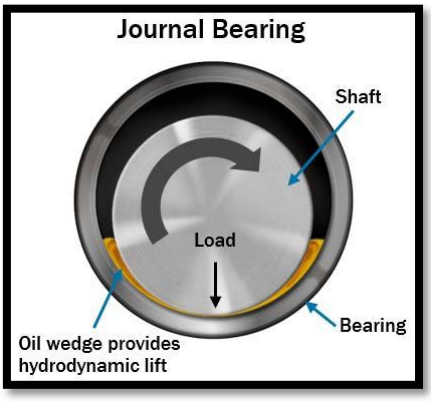

***Fig. 2.9** Bearing and shaft [16]*

2.5. Tribological Tests

To gain information about the real tribological system in the area of friction, wear and lubricating, there are quite a lot of different tribological tests at disposal. However, the real tribo-system (under manufacturing conditions) is quite complicated because it is influenced by many factors (e.g. microgeometry, substrate, lubricant, etc). Moreover, these factors not only influence the tribology system, but they are influencing each other. To take into account such complexity of the real tribological system, specific conditions have to be ensured already during the laboratory testing. Nevertheless, such testing is performed more on the micro model level and as a measured data there are outer measured quantities. Among them belongs mainly the measurement of the drawing force (F_T). In Fig. 2.10 are shown the basic tribological tests and some of them are described on the next pages. [17, 18]

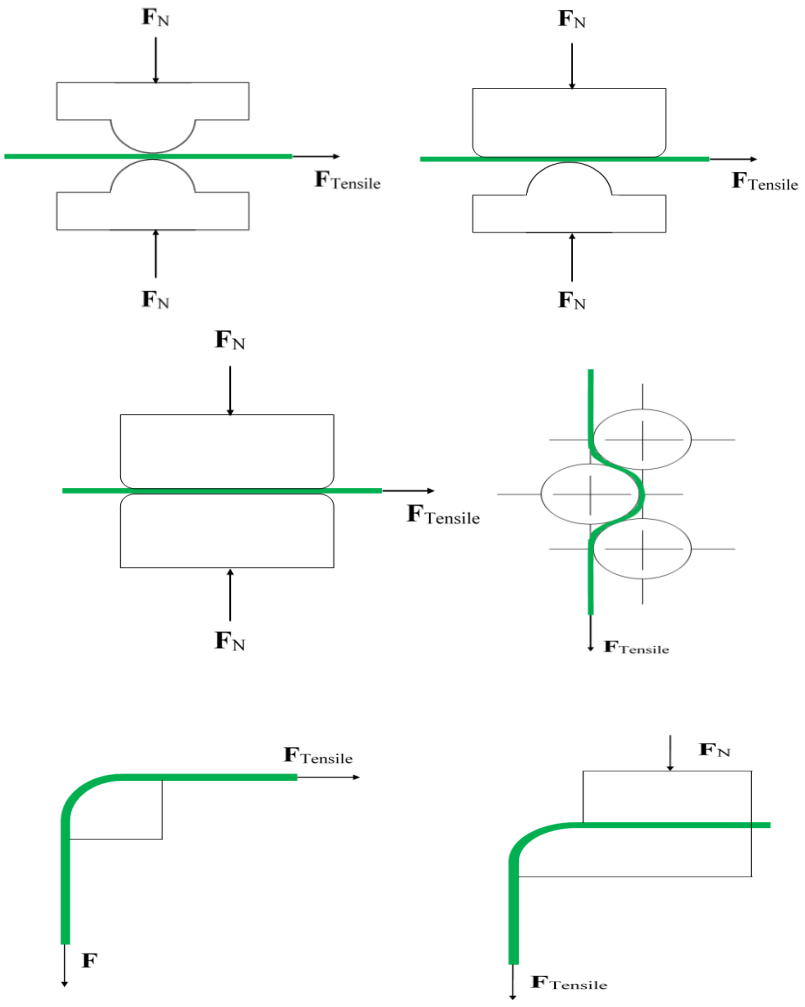

Fig. 2.10 *Schematic of basic tribological tests [4]*

2.5.1. Tribological Process in the Blank Holder

In this process the sample as strip is clamped between the blank holder and it is drawn by a force called drawing force F_T [N]. The contact pressure p [MPa] is applied on both sides of the sample, so while calculation there is multiplication of contact pressure by 2. The schematic diagram of this process is shown in Fig. 2.11 and own calculation of the friction coefficient is done by using the formula (4). Moreover, this kind of tribological test was subsequently used in the experimental part of this thesis.

$$\mu_1 = \frac{F_{T1}}{2.p.s} \tag{4}$$

where:

s	-	contact area	[mm$^{2]}$
p	-	contact pressure	[MPa]
F_{T1}	-	drawing force	[N]
μ_1	-	friction coefficient in the blank holder area	[1]

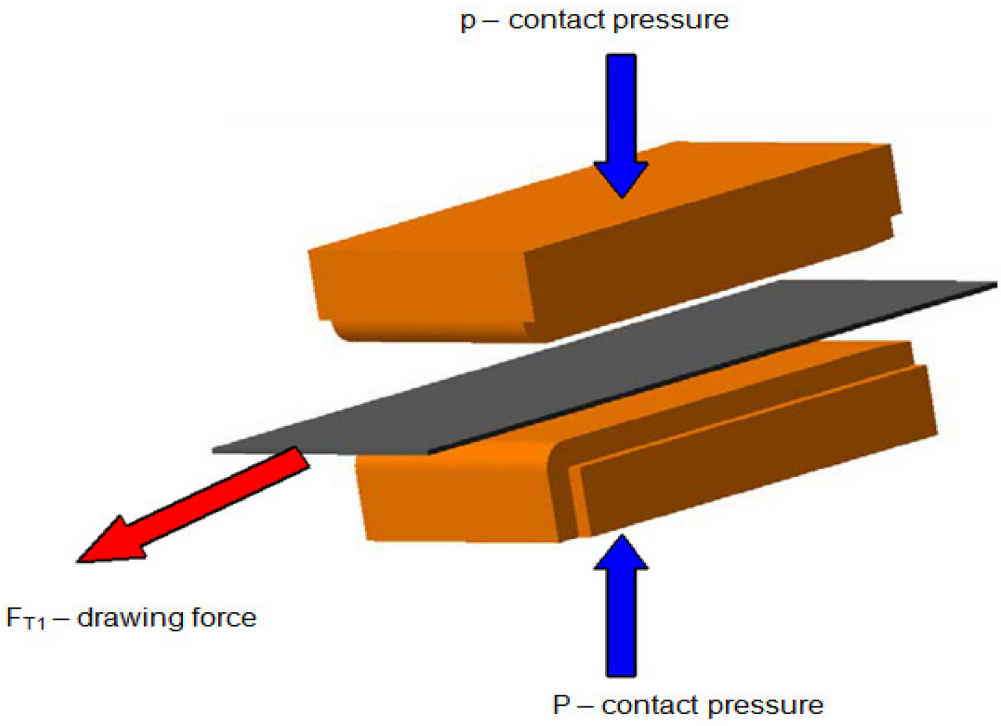

Fig. 2.11 *Strip drawing test - simulation in the blank holder area*

2.5.2. Tribological Process in the Drawing Edge

In this process is (as in the previous one) sample placed between the clamps and there is a rotating roller on the edge of one clamp. The drawing of the sample is made under 90° to bend the testing strip. The schematic of the above explanation is shown in Fig. 2.12 and calculation of bending force F_0 [N] is using the formula (5):

$$F_O = F_{T2} - F_{T1} \tag{5}$$

Where:

F_o - bending force on the drawing edge [N]

F_{T2} - drawing force after bending [N]

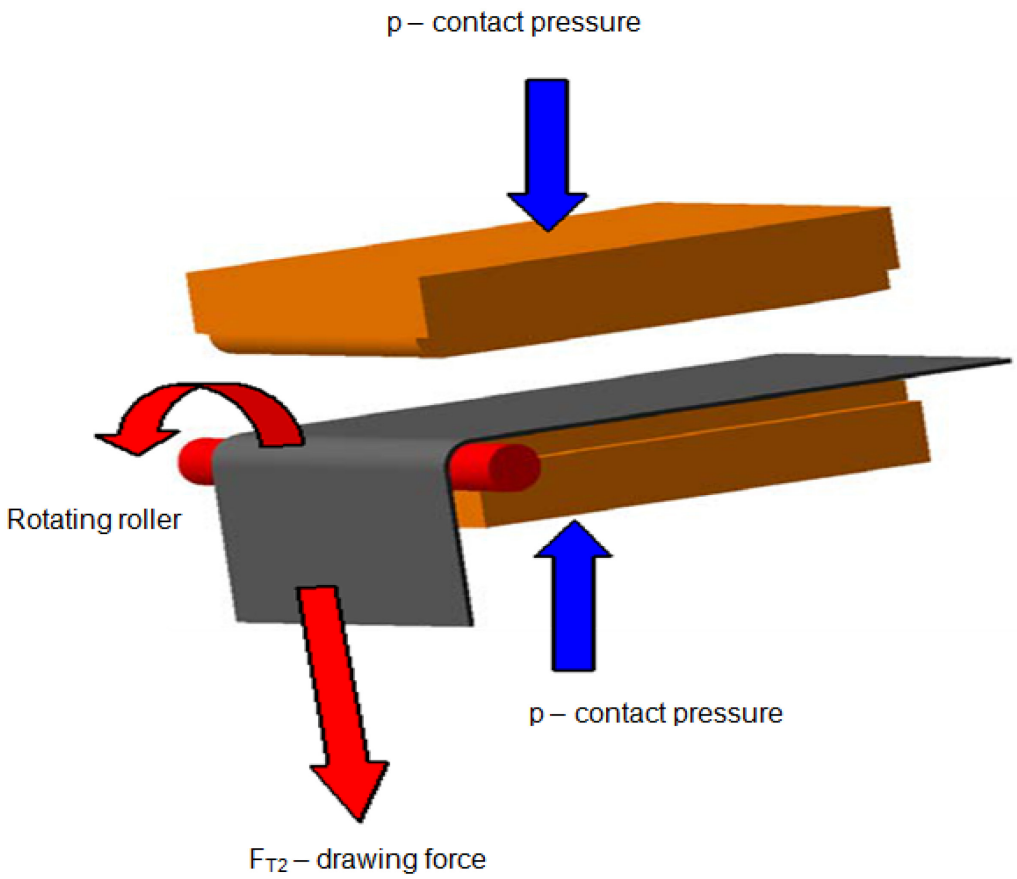

Fig. 2.12 *Strip drawing test – simulation of bending force on the drawing edge*

2.5.3. Tribological Process in the Blank Holder Area

In this process the drawing strip is placed between the clamps and there is no rotating wheel at the bending edge. The drawing force F_{T3} [N] is applied under 90° and the sheet is bent again (here without roller). The schematic of this process is shown in Fig. 2.13 and calculation of the drawing force is done via equation (6).

$$F_{T3} = F_O + F_{T1}.e^{\alpha.\mu 2} \tag{6}$$

Where:

F_{T3}	-	drawing force after bending	[N]
α	-	angle of contact (here π/2)	[1]
μ_2	-	friction coefficient on the drawing edge	[1]

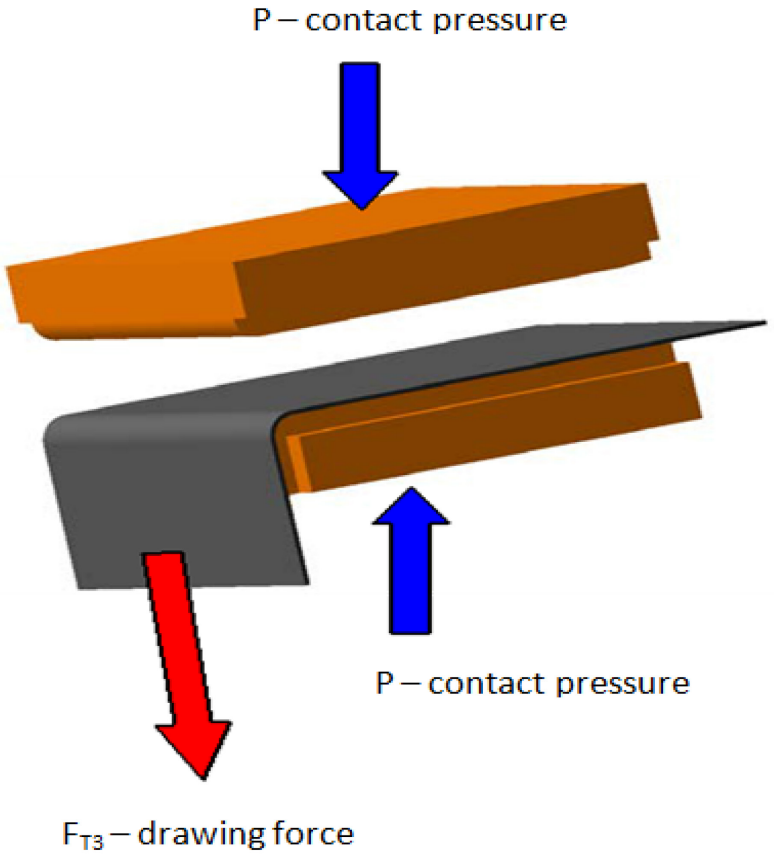

Fig. 2.13 *Strip drawing test – simulation of drawing force after bending*

3. MATERIALS FOR CAR-BODY DESIGN

The materials used for car-body design are discussed in this chapter (mainly there are described deep-drawing steels regarding the experimental part).

3.1. Material Selection Criteria

The materials that are to be used at car-body design are shown in Tab. 3.1. As major parameters there are their mechanical and physical properties. Steel is the most commonly used material by any manufacturer because it has ease of process ability and compatible facilities. Besides that, aluminium and magnesium is also considered at the car-body design. Moreover, some polymer materials are also used together with the composites (mostly in competition vehicles). [19, 20]

Tab. 3.1 *Overview of selected materials for car-body [19]*

Material	**Design parameters**					**Ease of manufacturing ('process chain')***		
	Yield strength σ_y **[MPa]**	Ultimate tensile strength σ_m **[MPa]**	Total ductility A_{80mm} **[min%]**	Young's modulus **E [GPa]**	Density **ρ [g.cm^{-3}]**	Forming	Joining	Paint
Forming grade steel EN 10130 DCO4 +Z	140 min	270 min	40	210	7.87	8	9	9
HSS EN 10292 H300YD +Z	300 min	400 min	26	210	7.87	6	8	9
UHSS - martensitic	1050-1250	1350-1550	5	210	7.87	4	7	9
Aluminium 5xxx	110 min	240 min	23	69	2.69	6	5	8
Aluminium 6xxx	120 min	250 min	24	69	2.69	6	5	8
Magnesium sheet	160 min	240 min	7	45	1.75	4	4	7
Titanium sheet	880 min	924 min	5	110	4.50	6	5	7
Glass fiber reinforced polymer	950	400-1800	<2.0	40	1.95	8	7	8
Carbon fiber reinforced polymer	1100	1200-2250	<2.0	120-250	1.60-1.90	8	7	8
*Based on range: 1 = difficult to process; 10 = production without difficulty								

3.1.1. Consistency of Materials

Including materials physical and mechanical properties, an important requirement is that consistency in the manufacturing process. Once a part is set to operate within its mechanical, physical and dimensional specifications, there should not be any disruptions like reset process variables as e.g. press and weld settings are. Material characteristics must be uniform to achieve the full benefits. Especially in the automatic manufacturing process, some defective process may lead to a large quantity of scrap before the fault is detected. So, continuous monitoring of production is important. Uniformity and the highest possible quality must be the twin aims. [20]

In manufacture of steel, continuous casting and annealing process are widely introduced everywhere. Casting of thin section dimension is also becoming reality nowadays. In aluminium industry also continuous casting and annealing has been developed. In chapters below, the basic materials used in automotive industry are explained. [21]

3.2. Steel

In contrary to the research that has been carried out for the last 30 years to develop a light weight material, most of the car body structure is built of steel. It requires half ton of flat rolled steel to produce the car-body. Steel has exceptional properties in terms of formability strength and cost. It is also easier to adapt to changing engineering needs and environmental requirements. The major advantages of steel are:

- low cost,
- ease of forming and joining,
- consistency of supply,
- corrosion resistance with coatings,
- recyclability,
- good crash energy absorption.

Among the disadvantages are:

- it is heavier than alternative materials,
- it can corrode if uncoated. [20]

The range of steels that are used in the automotive design varies a lot - from forming grades with a minimum yield of 140 MPa up to ultra-high strength steels (UHSS) with yield values about 1200 MPa. Their basic types are listed in Tab. 3.2. Before 10 years, corrosion was an important issue for these materials, but nowadays zinc coated, electro-galvanized, hot dip galvanized steels, alloyed and duplex materials have overcame this issue. Generally, these materials have some range of steel properties for normal forming and high-strength grades, but with hot dip galvanized sheet there may be slight reduction in ductility due to effect of the heat treatment cycle. [19]

Tab. 3.2 *Basic flat rolled steel product variants [19]*

BH	Bake-hardenable
CMn	Carbon-Manganese
CP	Complex phase
DP	Dual phase
HSLA	High-strength low-alloy
IF	Interstitial free
MART	Martensitic
MILD	Mild steel
SS	Stainless steel (austenitic)
TRIP	Transformation induced plasticity
TWIP	Twinning induced plasticity

3.2.1. Ultra High-Strength Steels (UHSS)

Most of the designers are using steels having Ultimate Tensile Strength (UTS) values up to or even over 1200 MPa, in order to reduce front and rear impact loads and also as B/C posts, associated roof rails and door apertures to maximize side impact protection. Thus energy absorption is a key characteristic of these materials and is related to the stress-strain curve. Some common high strength steels are characterized in Tab. 3.3. [20]

Fig. 3.1 *Ultra high-strength steels [22]*

***Tab. 3.3** Basic types of UHSS [19]*

Type of flat rolled steels (1st two rows) or UHSS	Range of Yield stress σ_y [MPa]	Strengthening mechanism	Relevant standard
Low - carbon mild steel sheet Re-phosphorized	140-180 180-300	Residual C, Mn, Si Solid solution hardening	EN 10130 PrEN10xxxx EN 10292 (hot-dip zinc-coated)
Isotropic Bake - hardening	180-280 180-300	Si additions Strain age hardening	PrEN10xxxx PrEN10xxxx EN 10292 (hot dip zinc-coated)
High - strength Low - alloy	260-420	Grain refinement and precipitation hardening	PrEN10xxxx EN 10292 (hot dip zinc-coated)
Dual - phase	450-600 (UTS)	Martensitic (hard) phase in ferritic ductile matrix	PrEn 10xyz
TRIP steel	500-800	Transformation of retained austenite to martensite on deformation	PrEn 10xyz
Complex and martensitic steel	800-1200	Bainitic/martensitic (hard) phases formed by controlled heat treatment	PrEn 10xyz

Some advantages of the ultra-high strength steels are:

- **High strength** - ultra high strength steels are four times stronger than normal high strength steels (higher UTS or Yield strength, etc.).
- **Light weight** - compared to normal steel, ultra high strength steels can be formed 10 to 15% of more thin (thus weight reduction).
- **Shape ability** - some complex shapes can be achieved by ultra high strength steels. [20]

3.2.2. Stainless Steel

At these steels chromium is added to steel to form a protective film of the chromium oxide and increases the corrosion resistance. This material is not used in the current vehicles, but in commercial vehicles like buses. It has attractive forming parameters. Researchers are trying to re-examine this material to find a strong competitive advantage. These materials have high work hardening rates, critical loads can be approached with current working facilities. It has some demands like often inter stage annealing to achieve deep drawn shapes. The overall costs and changed processes may be unfavorable. But recent studies have made an alternative body architecture utilizing a stainless steel space frame and various bolt on assembly materials. [19]

Some of the advantages of stainless steels are:

- corrosion resistance,
- excellence formability,
- similar manufacturing characteristics as mild steel.

Some of its disadvantages are:

- its cost is high,
- the limited supply source for automotive applications.

3.2.3. Aluminium (Al)

Aluminium is known for its low density which is ρ_{Al} = 2.69 g·cm^{-3}. By the rule of thumb the alternative to steel, the weight can be halved but the cost will get doubled. The density of aluminium is one third of steel, but its modulus (E_{Al} = 69 GPa) is very low compared to steel (E_{Steel} = 210 Gpa). Because the required stiffness cannot be achieved, thickness of some parts is increased. The cost may be higher and it gets fluctuated with rise and fall of commodity markets. Thus for planning purpose some means of stabilizing future costs (such as buying ahead or an alternative strategy) must be considered. Since the cost is higher, the total manufacture cost is also higher, such as the need for modification of the welding equipment, faster electrode tip wear and need for additional changes to paint process. In recent days one important disadvantage of aluminium is expensive repair of specialist parts such as cast nodes, which could make difficulty in higher insurance premium locating a specialist repair shop. [19]

Some advantages of aluminium are:

- low density,
- corrosion resistance,
- strong supply base,
- recyclability.

Some disadvantages are listed below:

- high and fluctuating cost,
- worse formability than steel,
- less readily welded than steel.

3.2.4. Magnesium (Mg)

In the list of engineering metals, magnesium is the lightest metal of all. It has a density of 1.74 g·cm^{-3}, which is 35% lower than aluminium and four times lower than steel. It is produced by the metallothermic reduction of magnesium oxide with silicon or electrolysis of magnesium chloride melts from sea water. It is said that one cubic meter of sea water contains 1.3 kg of magnesium.

Magnesium alloys are the combination of magnesium (Mg), aluminium (Al), manganese (Mn) and zinc (Zn). Their composition and basic properties are shown in Tab. 3.4. The higher elongation levels of the AM60 and AM50 means that they may be preferred over AZ91. These alloys have high purity with lower levels of heavy metal impurities (e.g. Fe, Cu or Ni) and have vastly improved corrosion resistance.

Tab. 3.4 *Automotive magnesium alloys [20]*

Magnesium alloy	**AZ91**	**AM60**	**AM50**
Composition (wt%)			
Al	9	6	5
Zn	0.7		
Mn	0.2	0.3	0.3
Typical RT properties			
UTS [MPa]	240	225	210
Yield strength [MPa] (0.2% offset)	160	130	125
Final ductility [%]	3	8	10

Some advantages of magnesium are:

- low density,
- ability to be thin casted,
- possibility to integrate components in castings.

Its disadvantages include:

- mostly available as cast components,
- high cost at medium to high volumes. [19]

3.3. Polymers and Composites

Thermoplastics and thermosets are the two divisions of polymers used for the car-body design. On the application of heat, thermoplastics melt because they are high molecular weight. Thermosets are irreversible materials in their nature, so they cannot be re-melted or re-formed. Reinforced plastics are mostly used as major composite materials in the car-body design. Composite materials have relatively high strength and low weight, excellent corrosion resistance, thermal properties and dimensional stability. Strength of polymer composites will increase with the percentage of fibrous material and is also affected by fiber orientation. [21]

3.3.1. Thermoplastics

Amorphous and crystalline ones are the two basic divisions of thermoplastics. In amorphous materials the molecules are not oriented in an orderly manner. Polycarbonate (PC) or acrylonitrile-butadiene-styrene (ABS) are just some of the amorphous thermoplastics - see Fig. 3.2. Some advantages and disadvantages of amorphous thermoplastics are tabulated in Tab. 3.5.

The molecules are arranged in orderly way in the crystalline thermoplastics. The processing technique and cooling rate is important for development of this structure. Polyamide (PA), polypropylene (PP) and polyethylene (PE) are some of the crystalline thermoplastics. [16]

Fig. 3.2 *Thermoplastic products [23]*

3.3.2. Thermosets

Compared to thermoplastics, thermosets are more brittle. So they are used with fiber reinforcement of some type. Thermosets are irreversible due to inter-bond between the molecules. Thermosetting polymers may be contrasted with thermoplastic polymers, which are commonly produced in pellets and shaped into their final product form by melting and pressing or injection molding. Some advantages and disadvantages of thermosets are given in Tab. 3.5. [19]

***Tab. 3.5** Basic advantages and disadvantages of polymers [19]*

Thermoplastics				**Thermosets**	
Amorphous		**Crystalline**		Advantages	Disadvantages
Advantages	Disadvantages	Advantages	Disadvantages		
Dimensionally stable	Poor wear abrasion and repeated impact	Good solvent, fatigue and wear resistance	Potentially high and variable shrinkage	Low sensitivity to temperature	Low toughness and strain at fracture
Lower mold shrinkage	Poor fatigue resistance	Higher design strain than amorphous grades	Difficult to adhesive bond	Good dimensional stability	Difficulties in recycling
Potential for application as structural foams	Increased process time	High temperature properties	Higher creep than amorphous thermoplastics	Harder and more scratch resistance	It is difficult to obtain info

***Fig. 3.3** Thermoset products [24]*

3.3.3. Composites

Composites are two or more materials with different physical or chemical properties, which reveal so-called synergic effect (mostly written as 1 + 1 = 3). They do not fully merge or dissolve into one another (see Fig. 3.4). Their basic parts are termed as termed as matrix and reinforcement. When additional strength is required, many types of plastics can be reinforced and it produces stronger materials, which are termed as composites. Composites are also referred to as fiber-reinforced polymer (FRP). FRP composite may contain:

- fillers,
- additives,
- core materials that modify and enhance the final product.

Beside engineering industry, composites are also used in the manufacture of e.g. sports equipment, aircraft, moulds for forming processes, etc. [19]

Fig. 3.4 *Composite products [25]*

Some advantages of composites are:

- they are light in weight,
- corrosion resistance,
- dimensional stability.

Some disadvantages of composites are:

- high cost,
- highly specialized manufacturing process required,
- cannot be easily recycled. [19]

4. SURFACE TREATMENT TECHNOLOGIES

Surface treatment of metals can be of essential importance in many industries like automotive industry, chemical industry, electrical industry, etc (see Fig. 4.1). It is not a new process. Surface treatment dates back as early as mankind started using gold decoratively approximately before 4000 BC. There are several reasons to change the properties of metals. The most important ones are as following [26]:

- decoration (or) reflectivity,
- improved hardness to resist damage and wear,
- prevention of corrosion.

Fig. 4.1 *Surface treatment of a car-body [27]*

Almost in every kind of industry, surface treatments are necessary – mainly in the following industries: automotive industry, construction industry, container industry, electrical industry, medical industry, industrial equipment, industries using laboratory equipment, aerospace and so on. Some the most common surface treatment technologies include [26]:

- chemical vapour deposition (CVD),
- chromadizing,
- electro-plating (electro-galvanizing),
- electro-polishing,
- flame hardening,
- hot dip galvanizing,
- induction hardening,
- physical vapour deposition (PVD).

4.1. Chemical Vapour Deposition (CVD)

CVD is generally a chemical process used to produce high-purity as well as high-performance solid materials. This technique is suitable for the production of coatings, powders, fibers and monolithic components. This technique is used in many thin film applications. By varying the experimental conditions (e.g. substrate material, substrate temperature, composition of the reaction gas mixture, total pressure gas flows), a lot of materials with different properties can be prepared.

CVD may be defined as the deposition of a solid on a heated surface from a chemical reaction in the vapour phase (see Fig. 4.2). It belongs to the class of vapour-transfer processes, which is atomistic in nature. It means that the deposition species are atoms or molecules or a combination of these. [28]

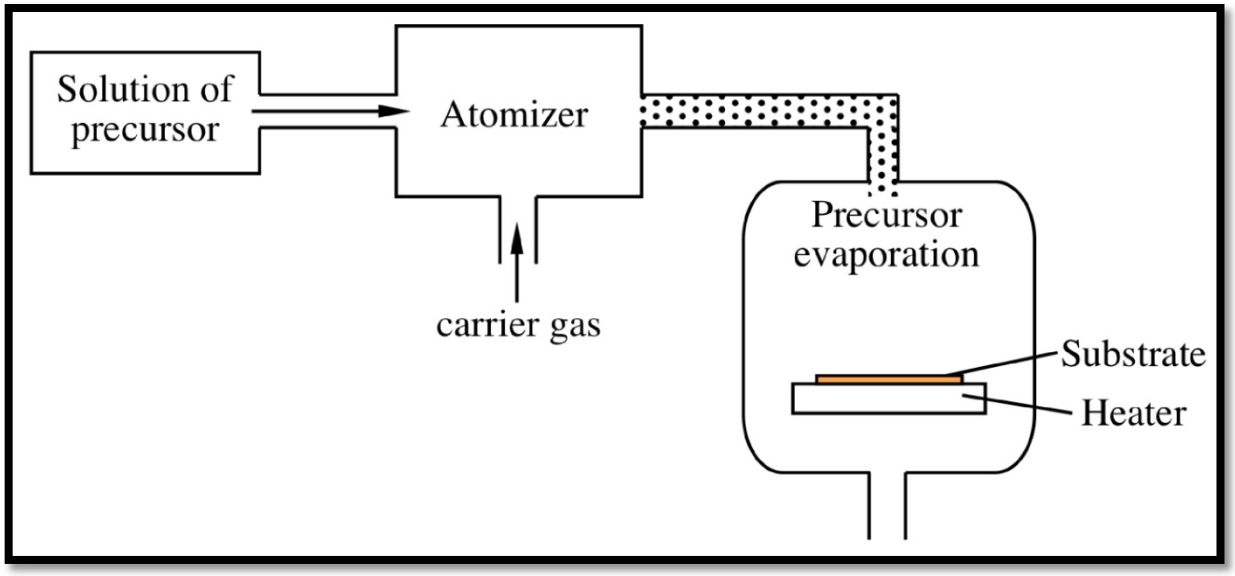

Fig. 4.2 *Schematic of chemical vapour deposition [29]*

The CVD is mostly classified according to:

- operating pressure,
- physical characteristics of vapour.

Some of the basic applications of CVD are:

- corrosion and wear resistant coatings,
- preparation of high temperature materials,
- metallurgical coatings industry,
- heat resistant coatings,
- production of novel powders and fibers.

4.2. Physical Vapour Deposition (PVD)

Physical Vapour Deposition (PVD) is a thin film coating process, which produces coatings of pure metals, metallic alloys and ceramics with a thickness usually within the range 1 to 10 μm. PVD involves physically depositing atoms, ions (or molecules) of a coating species onto a substrate (see Fig. 4.3). There are three main types of PVD techniques, all of which are undertaken in a chamber containing a controlled atmosphere with the reduced pressure (0.1 to 1 Nm^{-2}) [28]:

- thermal evaporation,
- sputtering,
- ion plating.

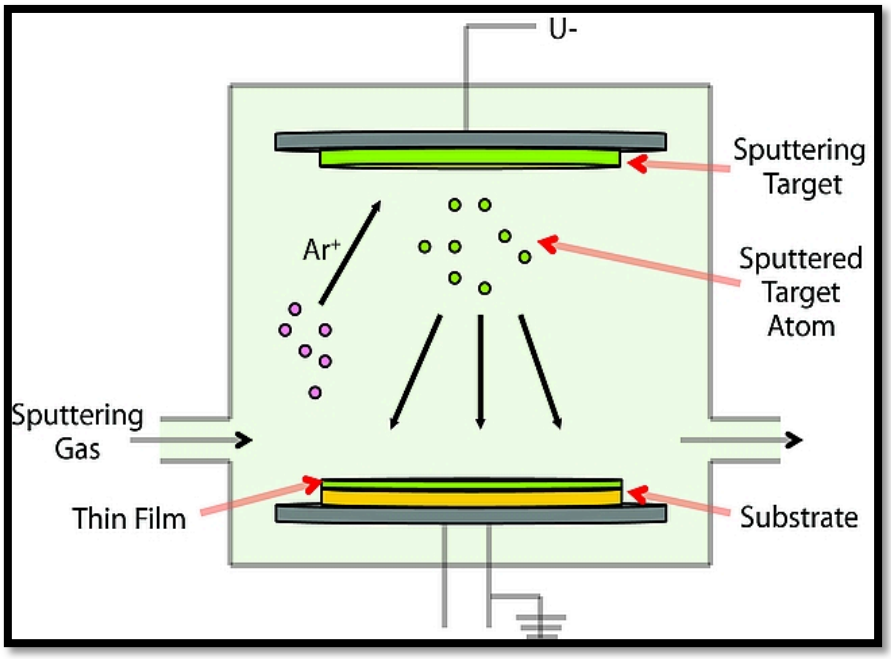

Fig. 4.3 *Schematic of physical vapour deposition [30]*

All three techniques can be used for the direct deposition of material for 'reactive' use in which chemical reaction occurs in the vapour (or plasma) phase between atoms of the coating material and 'reactive' gases [28].

Some of the applications of PVD are:

- corrosion resistance coatings,
- wear prevention coatings,
- decorative coatings on plastics.

4.3. Electro-Plating (Electro-Galvanizing)

Electro-plating is a common metal finishing process that is used in a number of industrial applications. It is also known as electro-deposition, which involves depositing a thin layer of metal onto the surface of a workpiece, which is referred as the substrate (see Fig. 4.4). The desired reaction is achieved by an electric current. For example, if a layer of gold is to be deposited onto the metal jewellery to improve the appearance of the piece, the plating metal (gold) in the case is connected to the anode (positively charged electrode) of the electric circuit, while the jewellery is placed at the cathode (negatively charged electrode). Both are immersed in a specially developed electrolytic solution (bath).At this point, DC current is supplied to the anode. It oxidizes the metal atoms in the gold and dissolves them into the bath. The dissolved gold ions are reduced at the cathode and deposited onto the jewellery product. Some commonly used metals for electroplating include zinc (Zn), copper (Cu), and tin (Sn), as well as precious metals such as gold (Au), silver (Ag) and palladium (Pd). [28]

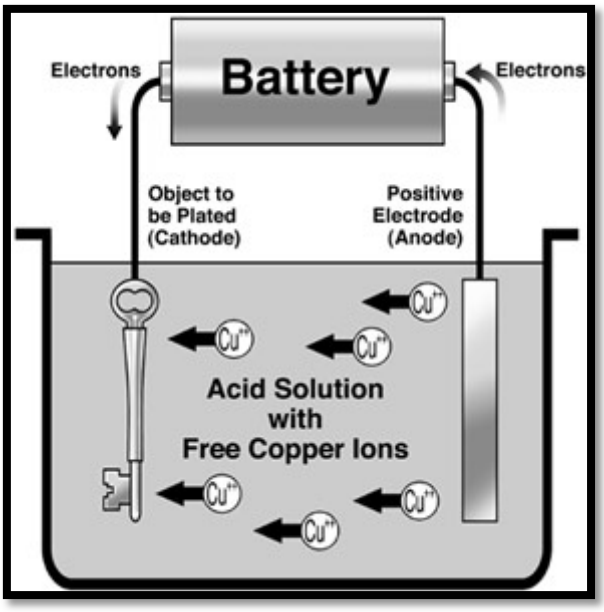

Fig. 4.4 *Electro-plating process [31]*

Some advantages of electroplating are:

- resistance to corrosion,
- increase of wear resistance,
- reducing friction,
- improving surface uniformity.

4.4. Hot Dip Galvanizing (HDG)

The hot dip galvanizing is a process of applying zinc coatings onto components made from steel or iron by immersing the component in a bath of molten zinc (see Fig. 4.5). The simplicity of the hot dip galvanizing process is a great advantage in comparison with other methods of corrosion protection.

Although the hot dip galvanizing is a very traditional process and its principle is not very complicated, it is necessary to consider conditions of cleanliness of the surface that is immersed in the zinc furnace. The crucial conditions to obtain a perfect quality of the final surface are [28]:

- all scale, oxides and corrosion product must be removed from the surface by pickling,
- the surface has to be activated,
- the perfect wettability of surface is to be reached by coating the surface with flux.

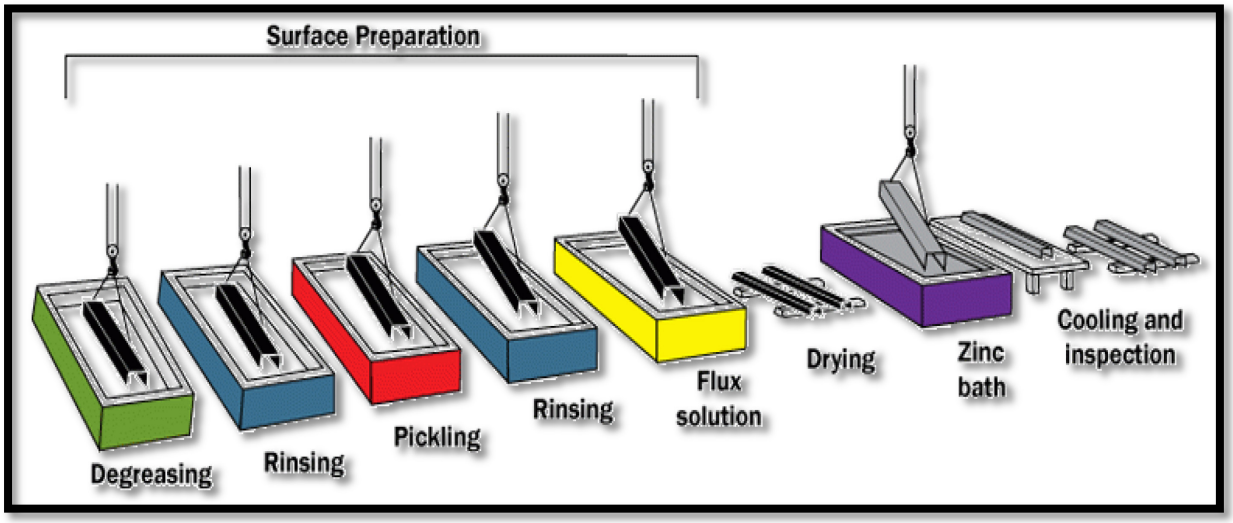

Fig. 4.5 *Hot dip galvanizing process [32]*

Some advantages of hot dip galvanizing are:

- strong and active barrier to corrosion,
- it is low of cost,
- zinc is safe for environment,
- ease of inspection,
- reliability,
- long life.

5. EXPERIMENTAL PART

In the experimental part of this thesis, two different samples of deep drawing steel was tested under the different tribological conditions. First set of samples is termed as Hot Dip Galvanized (HDG)samples and the second set of samples is generally termed as New Inorganic Treatment (NIT).Both of them are used in the automotive industry for car-body applications - mostly as outer panels. HDG sheets are generally used due to their good corrosion resistance and low price. On the other hand, NIT sheets represent still quite new coating type, which was developed by ArcelorMittal Ltd. It is a surface treatment, which improves the stamping behavior of all zinc based metallic coatings, especially under the high contact pressures. NIT is believed to offer properties and advantages to the current automobile production process by increasing productivity and scrap reduction. This additional property enhances the process reliability and can even lead to high cost savings.

After the preparation of samples (cut onto the required dimensions, degreasing and application of lubricant as Fuchs Anticorit PL 3802-39S of amount 1,5 $g \cdot m^2$), the strip drawing test (see Chap. 2.5.1) was performed under the different tribological conditions – see Tab. 5.1. The whole test was conducted under the software called Labnet to receive and evaluate measured data. After that, different types of forces (F_{max}, F_h, F_{avg}, ΔF, F_{min}) were firstly taken into account. Then, from the relevant kind of force (see Tab. 5.1), the corresponding friction coefficient μ [1] was computed.

Tab. 5.1 *Testing conditions and type of force used to compute friction coefficient*

<table>
<tr><td colspan="2">Contact pressure p [MPa]</td><td>8</td><td>23</td><td>38</td><td>53</td><td>68</td><td>83</td></tr>
<tr><td colspan="2">Feed rate v [mm/sec]</td><td>1</td><td>10</td><td>50</td><td>200</td><td>400</td><td></td></tr>
<tr><td rowspan="2">Type of force F [N]</td><td>HDG</td><td colspan="3">F_h</td><td colspan="3">F_{avg}</td></tr>
<tr><td>NIT</td><td colspan="2">F_h</td><td colspan="4">F_{avg}</td></tr>
</table>

As it is shown in the Tab. 5.1, for subsequent calculation of friction coefficient for HDG there was used F_h up to feed rate 50 mm/sec and then F_{avg} for 200 mm/sec and 400 mm/sec. In case of NIT, F_h was used only up to feed rate 10 mm/sec. After evaluation the friction coefficient for different samples, 3D color map surface graphs were created to give a very good overview and comparison of measured results.

5.1. Preparation of Samples

There were used two different surface treatments of samples in the tribological test of this thesis: the 1st one was common Hot Dip Galvanized (HDG) and the 2nd one was termed as New Inorganic treatment (NIT). Both of them were applied on the deep drawing material sample with thickness of 0.8 mm (Fig. 5.1 – left). The required width of the samples was 44.7 mm. So as the first step it was cutting of given samples to the required width by shearing tool (Fig. 5.1 – right).

Fig. 5.1 *Hot Dip Galvanized (HDG) sample (left) and shearing tool (right)*

The required dimension (44.7 mm) was set in the shearing tool and the sample was cut onto this magnitude with 90°ragarding rolling direction. Finally, there was cut about 40 samples for both tested substrates (see Fig. 5.2).

Fig. 5.2 *Samples after shearing (HDG– left, NIT - right)*

As there was already written before, samples with NIT substrate were also sheared in the same procedure with width 44.7 mm and the rolling direction 90° (see Fig. 5.2 – right). After that samples had the required dimensions (44.7 mm x 850 mm) and as the next step there was their degreasing and cleaning to remove old lubricants and dirty. This procedure is described on the next page.

To degrease the samples they were dipped into a chemical solution for about 2-3 hours to make sure that every minute particles are washed away by the solution. There was also used compressed air to make bubbles moving through the solution, thus to help degreasing process. The chemical solution bath is shown in Fig. 5.3

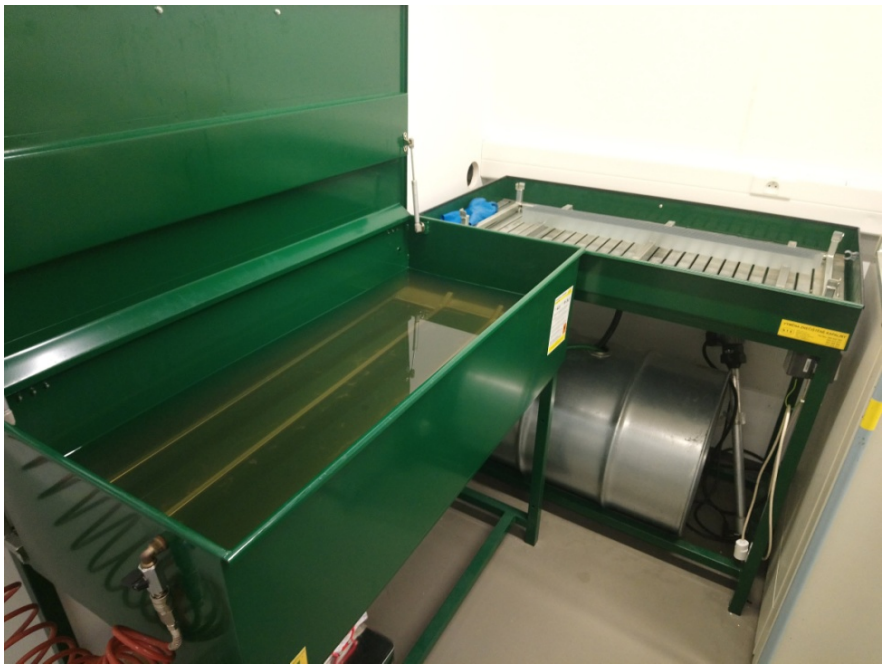

Fig. 5.3 *Degreasing solution bath for samples*

Then after the time period of 2-3 hours, the degreased set of samples was placed in a dryer (see Fig. 5.4) to make them dry.

Fig. 5.4 *Drying of samples after degreasing*

5.2. Tribological Testing- Strip Drawing Test at TUL

The own strip drawing test at TUL was carried out with a testing device shown in Fig. 5.5. The testing device is named as SOKOL 400 and consists of testing tool (here are placed testing jaws and whole testing method is adjusted here), load cell, moveable beam, hydraulic clamps, temperature aggregate, hydraulic aggregate and PC for evaluation tribological tests.

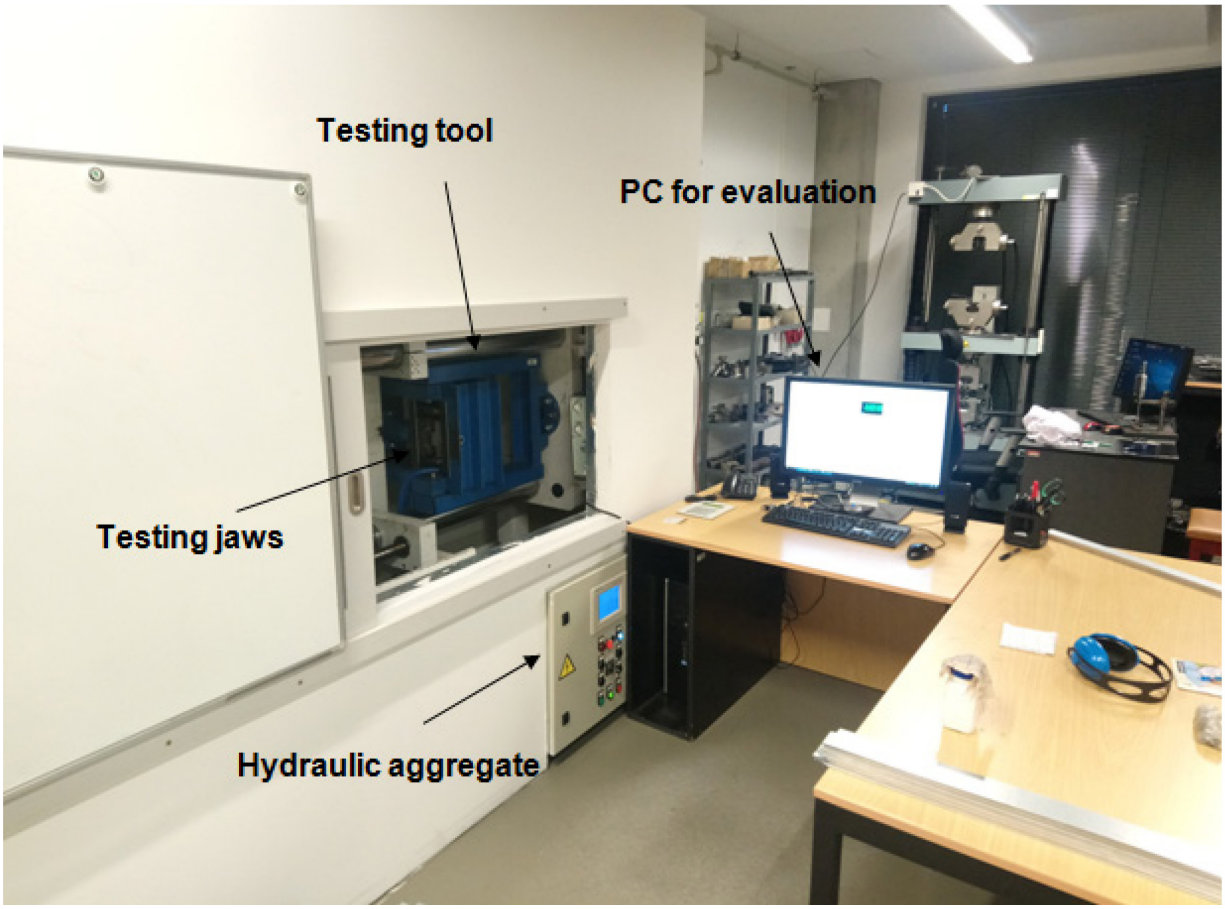

Fig. 5.5 *Tribological device (SOKOL 400) for strip drawing test*

A hydraulic aggregate was used to set the required contact pressure for the test in such way that the pressure was applied by the testing jaws placed in the testing tool. There was used also a temperature aggregate (not shown in Fig. 5.5) to maintain constant temperature for the tribological testing of samples. The temperature for the whole strip drawing test was 40°C.The PC shown in Fig. 5.5 was used to adjust the feed rate (it means velocity of sample) required for the strip drawing test and the tribological data were measured and obtained through the PC. The detail of the testing device is shown in Fig. 5.6. Here one can see also load cell, hydraulic clamps and column guiding. After every testing batch of samples, the contact pressure p [MPa] and feed rate v [mm/sec] were changed.

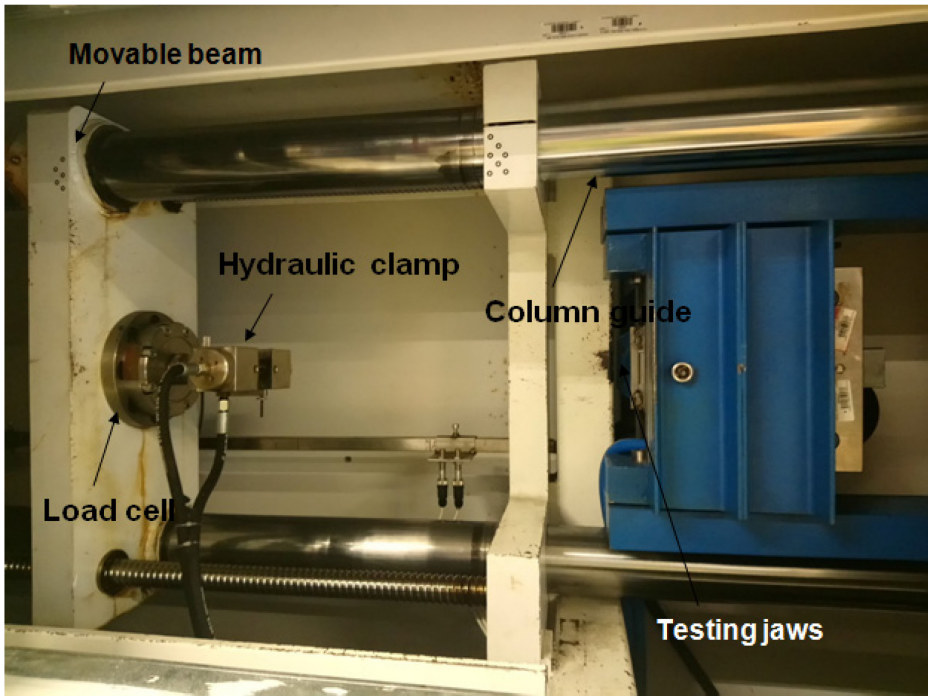

Fig. 5.6 *Detail of testing device*

Before the strip drawing test, the roughness parameters of HDG and NIT samples were measured (see Tab. 5.2). After that, samples to be tested were clamped between the hydraulic clamps and the testing jaws before the test was started. Then, the contact pressure p [MPa] and feed rate v [mm/sec] was adjusted (or checked) in the relevant aggregates. Finally, the test was started and the results were measured and obtained by PC. After that, own evaluation could start.

Tab. 5.2 *Surface roughness measurements*

Substrate	Roughness average	Peak count
	R_a[µm]	R_{Pc} [1/cm]
HDG	1,38/1,27	68/60
NIT	1,27/1,22	95/87

Evaluation and explanation of measured forces

Generally, there can be evaluated different types of measured forces during evaluation of the strip drawing test. The most important ones are as following:

F_{max}	-	maximal force	[N]
F_h	-	maximal force in stable zone	[N]
F_{min}	-	minimal force in stable zone	[N]
F_{avg}	-	average force	[N]
ΔF	-	peak-to-valley force (F_h-F_{min})	[N]

The own measured lengths both for HDG and NIT are given in Tab. 5.3. The measured length varied acc. to different feed rates. In this strip drawing test were used five feed rates as 1, 10, 50, 200, 400 mm/sec, resp.

Tab. 5.3 *Measured length for different feed rate*

Feed rate [mm/sec]	Measured length [mm]	Cut-off length [mm]
1	100	30
10	100	30
50	250	50
200	500	120
400	500	120

In light of different types of measured forces, the so-called cut-off length (thus also stable zone) is the most important factor. The stable zone in this test was considered as the zone after the cut-off length. F_{max} is primarily taken from the whole measured length but forces as F_h, F_{min} and F_{avg} are taken just from the stable zone (after cut-off length). The values of cut-off length are shown in Fig. 5.7. This graph corresponds to substrate HDG, feed rate 400 mm/sec and contact pressure 68 MPa. Right in this graph is cut-off length of 120 mm. The stable area is after the cut-off length and after the cut-off length (in the stable zone) forces like F_{max}, F_{min}, F_{avg}, were evaluated. The maximal force in the stable zone (F_h)is quite important, because it is generally used to compute the friction coefficient.

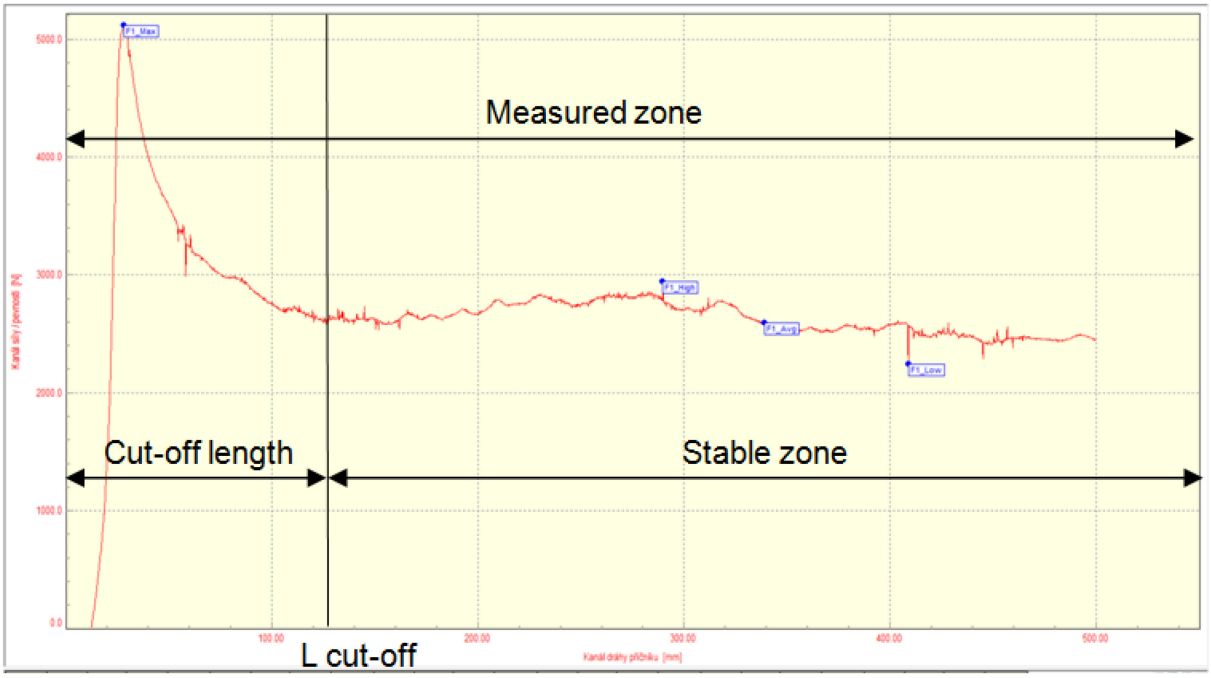

Fig. 5.7 *Measured forces after the cut-off length*

5.3. Measured Results– HDG and Feed Rate v = 1 mm/sec

Results measured by means of the strip drawing test were subsequently tabulated and graphs were done to compare all important results. Because of the space and better overview, results only for the HDG and feed rate v = 1 mm/sec are shown in this chapter. So in the Tab. 5.4 are shown results (acc. to different types of forces) for substrate HDG, feed rate v =1mm/sec and contact pressure p = 8 MPa. The corresponding graph for this table is shown in Fig. 5.8.

Tab. 5.4 *Measured forces for HDG, 1 mm/sec and 8 MPa*

Measured forces	Substrate	Feed rate	Contact Pressure		
	HDG	**1 mm/sec**	**8 MPa**		
No.	**F_{max} [N]**	**F_h [N]**	**F_{Avg} [N]**	**F_{min} [N]**	**ΔF [N]**
1	1441	1411	977	743	468
2	1448	1448	977	747	461
$\bar{x}$	**1440**	**1440**	**977**	**745**	**465**
s	2	2	0	3	5

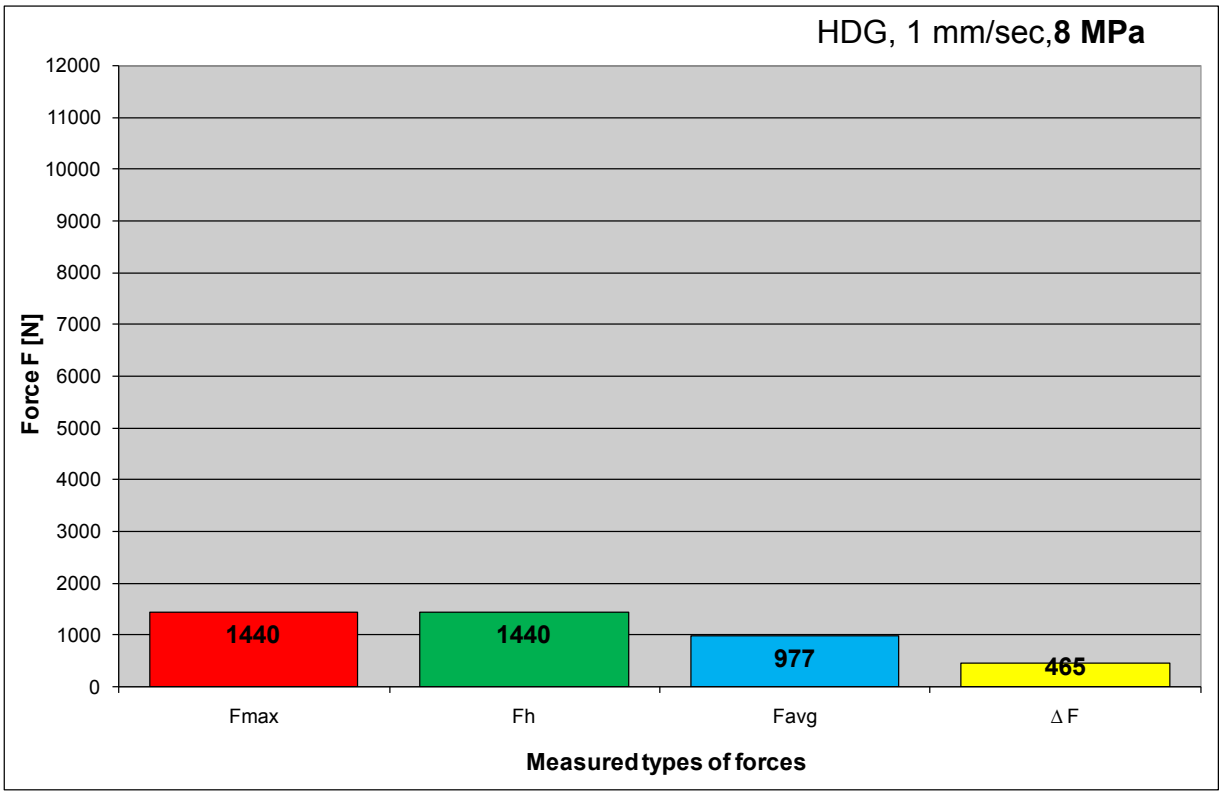

Fig. 5.8 *Measured forces for HDG, 1 mm/sec and 8 MPa*

In the Tab. 5.5 are shown results for HDG, feed rate v = 1mm/sec and contact pressure p = 23 MPa. The corresponding graph for these conditions is subsequently shown in Fig. 5.9. From the comparison of results for contact pressures 8 MPa and 23 MPa, it is obvious that forces F_h, F_{max}, F_{avg} increased cca. By 20%. Note mainly the values of important peak-to-valley forces ΔF (465 N for p = 8 MPa and 1906 N for p = 23 MPa), which means that under tested contact pressure (23 MPa), undesirable stick-slip effect takes place that can finally lead to galling of Zn layer.

Tab. 5.5 *Measured forces for HDG, 1 mm/sec and 23 MPa*

Measured forces	Substrate	Feed rate	Contact Pressure
	HDG	**1 mm/sec**	**23 MPa**

No.	**F_{max} [N]**	**F_h [N]**	**F_{Avg} [N]**	**F_{min} [N]**	**ΔF [N]**
1	3483	3374	2229	1315	1829
2	3660	3516	2295	1303	1983
$\bar{x}$	**3575**	**3445**	**2262**	**1309**	**1906**
s	129	100	47	8	109

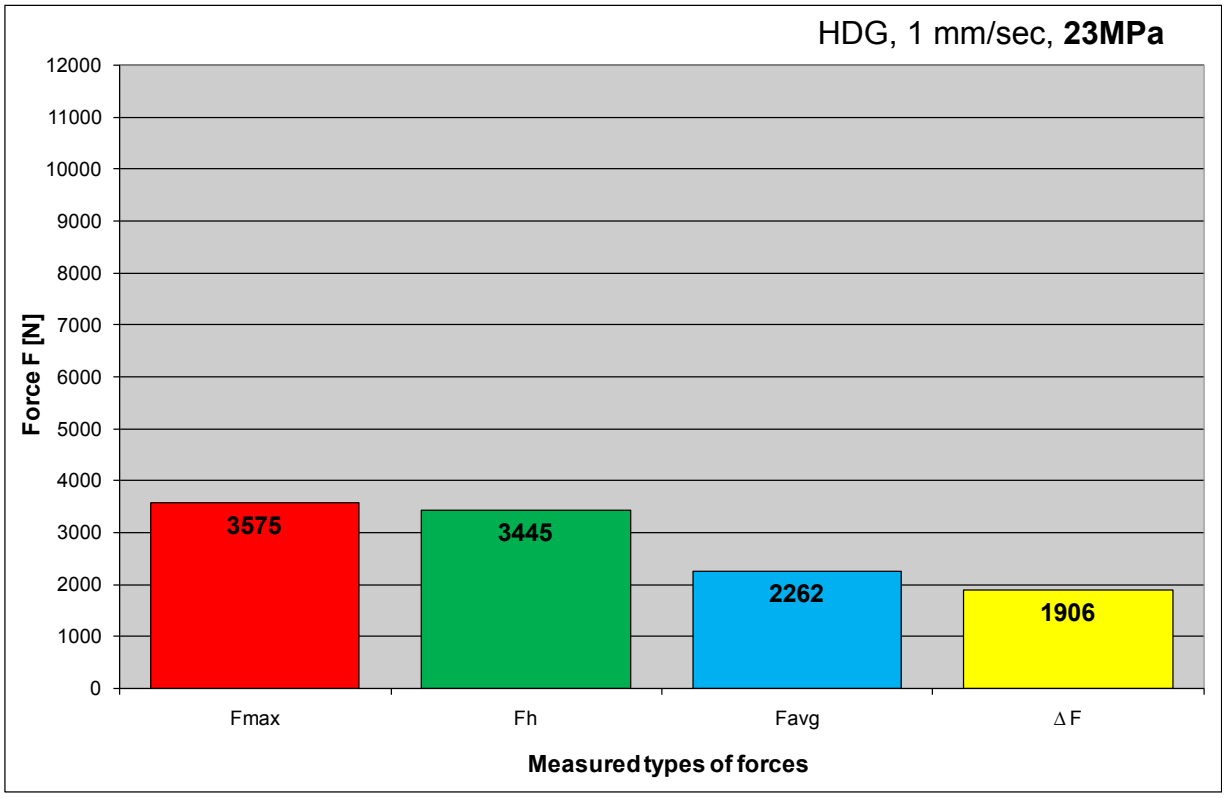

Fig. 5.9 *Measured forces for HDG, 1 mm/sec and 23 MPa*

In the Tab. 5.6 are shown results for HDG, feed rate v = 1mm/sec and contact pressure p = 38 MPa. The corresponding graph for these conditions is subsequently shown in Fig. 5.10. In light of basic results, forces F_h, F_{max}, F_{avg} increased approx. by 50% of results for p = 23 MPa. Quite important peak-to-valley force ΔF is now about 2-times higher than in the previous case. Note that F_{max} and F_h are again equal as in the first case (8 MPa), which means that maximal force was measured in the stable zone – mainly at the end of whole measured length.

Tab. 5.6 *Measured forces for HDG, 1 mm/sec and 38 MPa*

Measured forces	Substrate	Feed rate	Contact Pressure
	HDG	**1 mm/sec**	**38 MPa**

No.	**F_{max} [N]**	**F_n [N]**	**F_{Avg} [N]**	**F_{min} [N]**	**ΔF [N]**
1	5407	5407	3656	1904	3503
2	5498	5498	3793	2087	3411
$\bar{x}$	**5453**	**5453**	**3725**	**1996**	**3457**
s	64	64	97	129	65

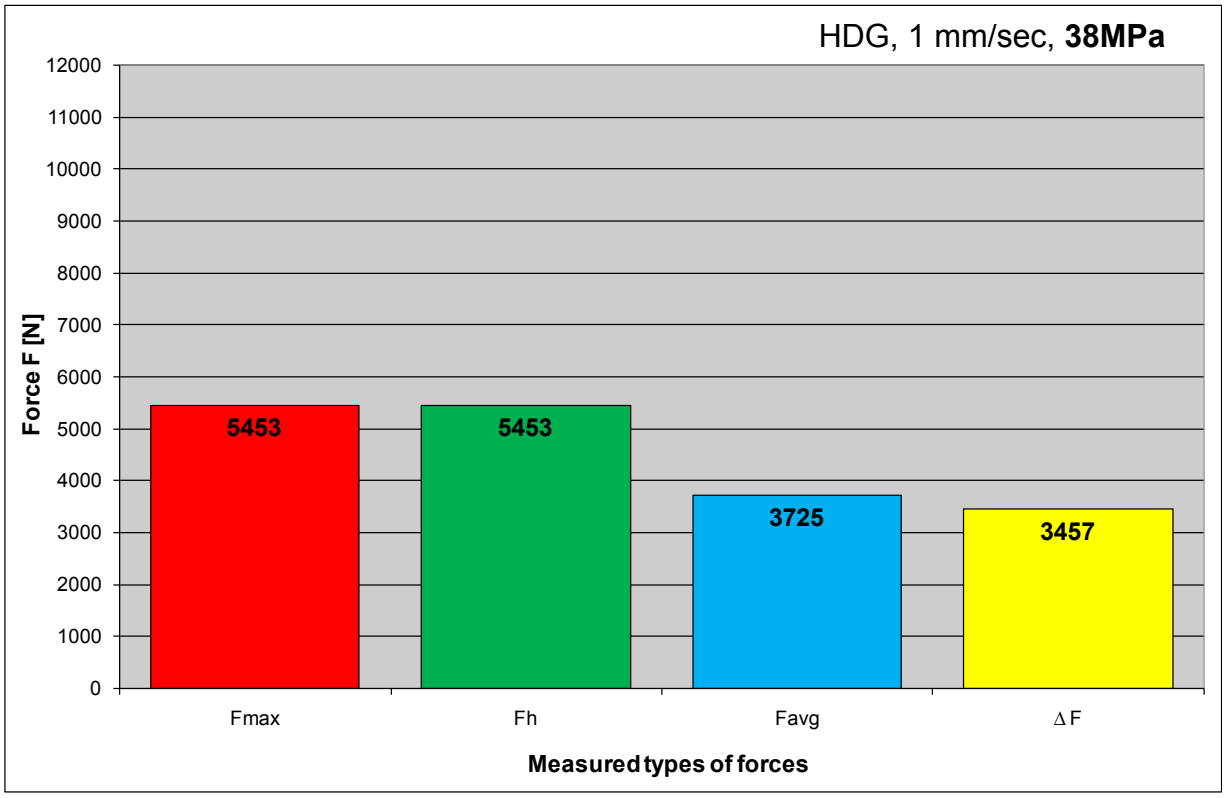

Fig. 5.10 *Measured forces for HDG, 1 mm/sec and 38 MPa*

In the Tab. 5.7 are shown results for HDG, feed rate v = 1mm/sec and contact pressure p = 53 MPa. The corresponding graph for these conditions is subsequently shown in Fig. 5.11. Compared again to the previous case, now are forces F_{max} and F_h higher approx. by 40%. Much higher increase was here measured for force ΔF, namely 60%. That is already quite severe magnitude, which can cause a heavy damage of tested material surface by galling. Generally, higher contact pressure means higher forces and that´s why the increase rate is important to be evaluated.

Tab. 5.7 *Measured forces for HDG, 1 mm/sec and 53 MPa*

Measured forces	Substrate	Feed rate	Contact Pressure
	HDG	**1 mm/sec**	**53 MPa**

No.	**F_{max} [N]**	**F_h [N]**	**F_{Avg} [N]**	**F_{min} [N]**	**ΔF [N]**
1	7895	7862	4888	2146	5486
2	7845	7845	4862	2109	5506
$\bar{x}$	**7870**	**7854**	**4875**	**2128**	**5496**
s	35	12	18	26	14

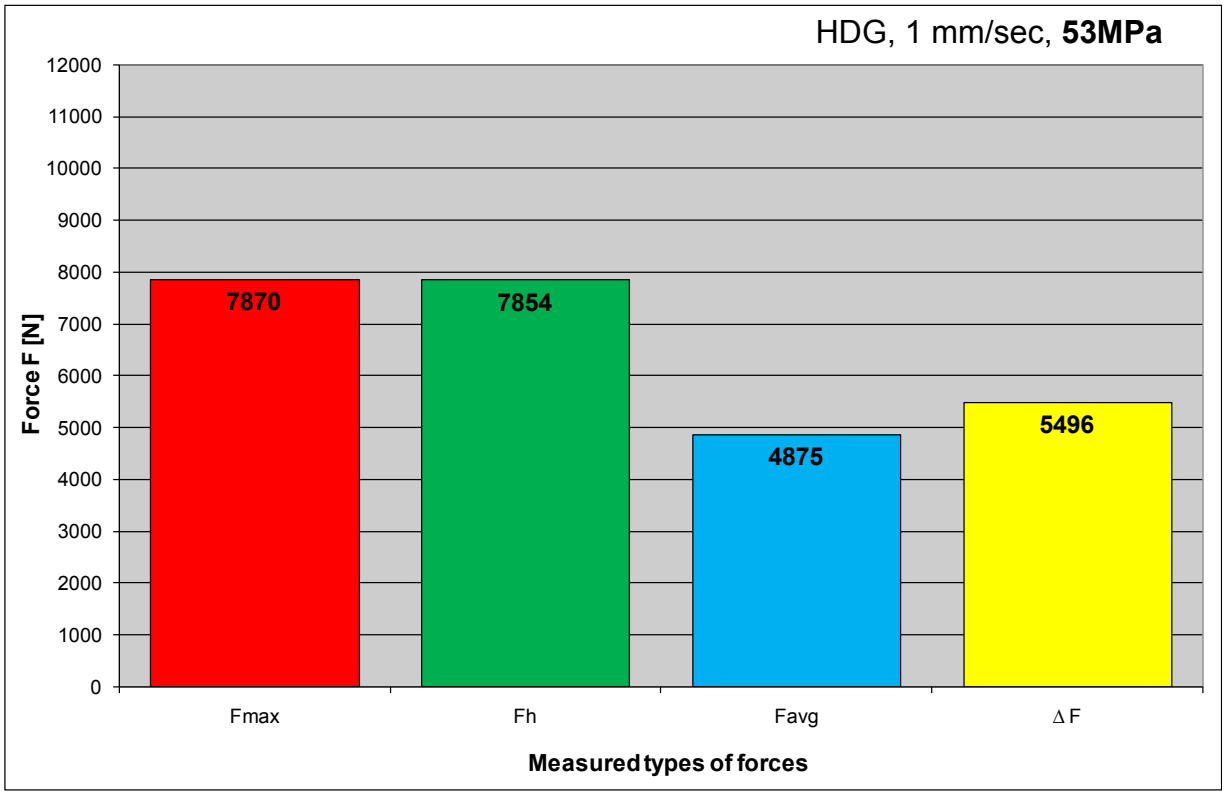

Fig. 5.11 *Measured forces for HDG, 1 mm/sec and 53 MPa*

In the Tab. 5.8 are shown results for HDG, feed rate v = 1mm/sec and contact pressure p = 68 MPa. The corresponding graph for these conditions is subsequently shown in Fig. 5.12. Such magnitude of contact pressure (p = 68 MPa) is already quite high and values of measured forces correspond to it. Note that F_{max} was measured in the stable zone (not at the beginning, because $F_{max} = F_h$), which means that force values were still increasing a little in dependence on measured length. Value of ΔF increased by another 50% compared to previous contact pressure.

Tab. 5.8 *Measured forces for HDG, 1 mm/sec and 68 MPa*

Measured forces	Substrate	Feed rate	Contact Pressure
	HDG	**1 mm/sec**	**68 MPa**

No.	**F_{max} [N]**	**F_h [N]**	**F_{Avg} [N]**	**F_{min} [N]**	**ΔF [N]**
1	10392	10392	6121	2080	8082
2	10478	10478	6131	2013	8235
$\bar{x}$	**10435**	**10435**	**6126**	**2047**	**8159**
s	61	61	7	47	108

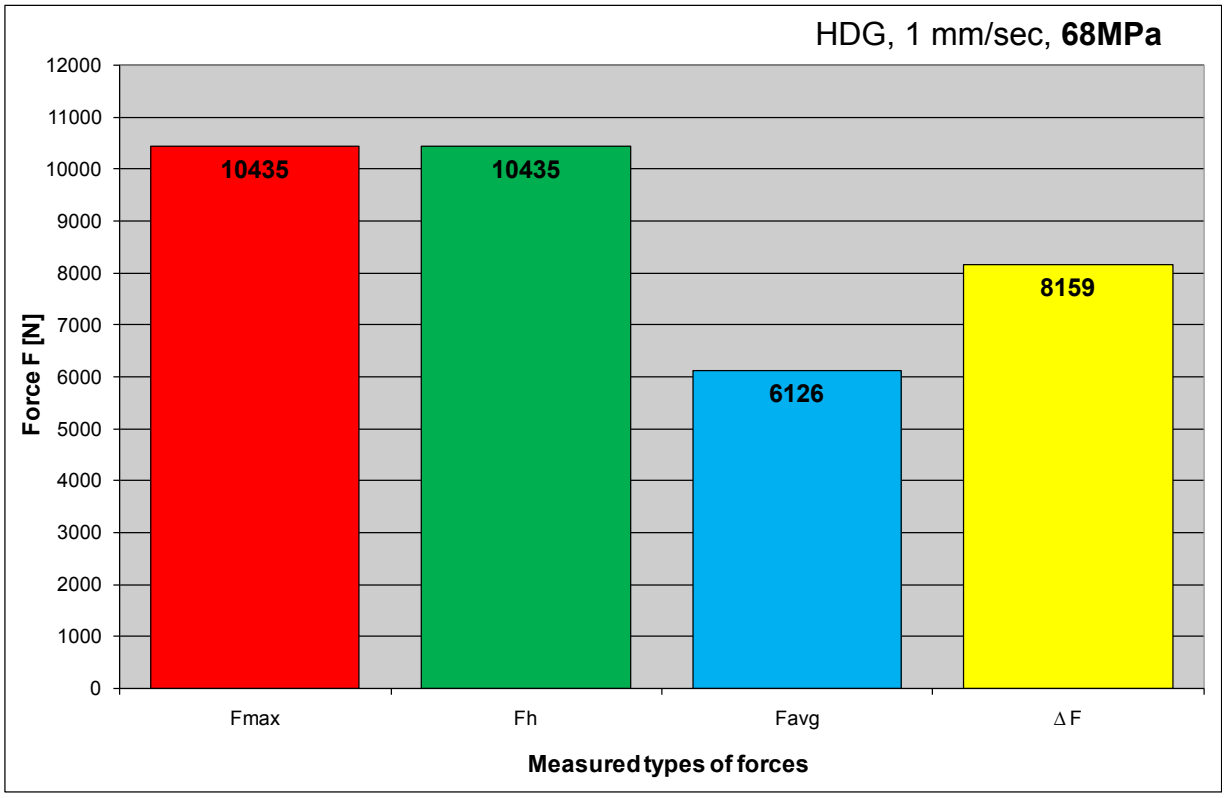

Fig. 5.12 *Measured forces for HDG, 1 mm/sec and 68 MPa*

In the Tab. 5.9 are shown results for HDG, feed rate v = 1mm/sec and the highest applied contact pressure p = 83 MPa. The corresponding graph for these conditions is subsequently shown in Fig. 5.13. Forces F_{max} and F_h are already over 12 000 N, which can result in plastic deformation of sample. Generally speaking, there is common static tensile test (just without strain gauge) from strip drawing test. In this case, all samples "survived without fracture", but they revealed truly very high values of forces. After this 1st evaluation, friction coefficient μ [1] was computed.

Tab. 5.9 *Measured forces for HDG, 1 mm/sec and 83 MPa*

Measured forces	Substrate	Feed rate	Contact Pressure
	HDG	**1 mm/sec**	**83 MPa**

No.	**F_{max} [N]**	**F_h [N]**	**F_{Avg} [N]**	**F_{min} [N]**	**ΔF [N]**
1	12304	12281	6992	1933	10118
2	12093	12061	6847	1863	9968
$\bar{x}$	**12199**	**12171**	**6920**	**1898**	**10043**
s	149	156	103	49	106

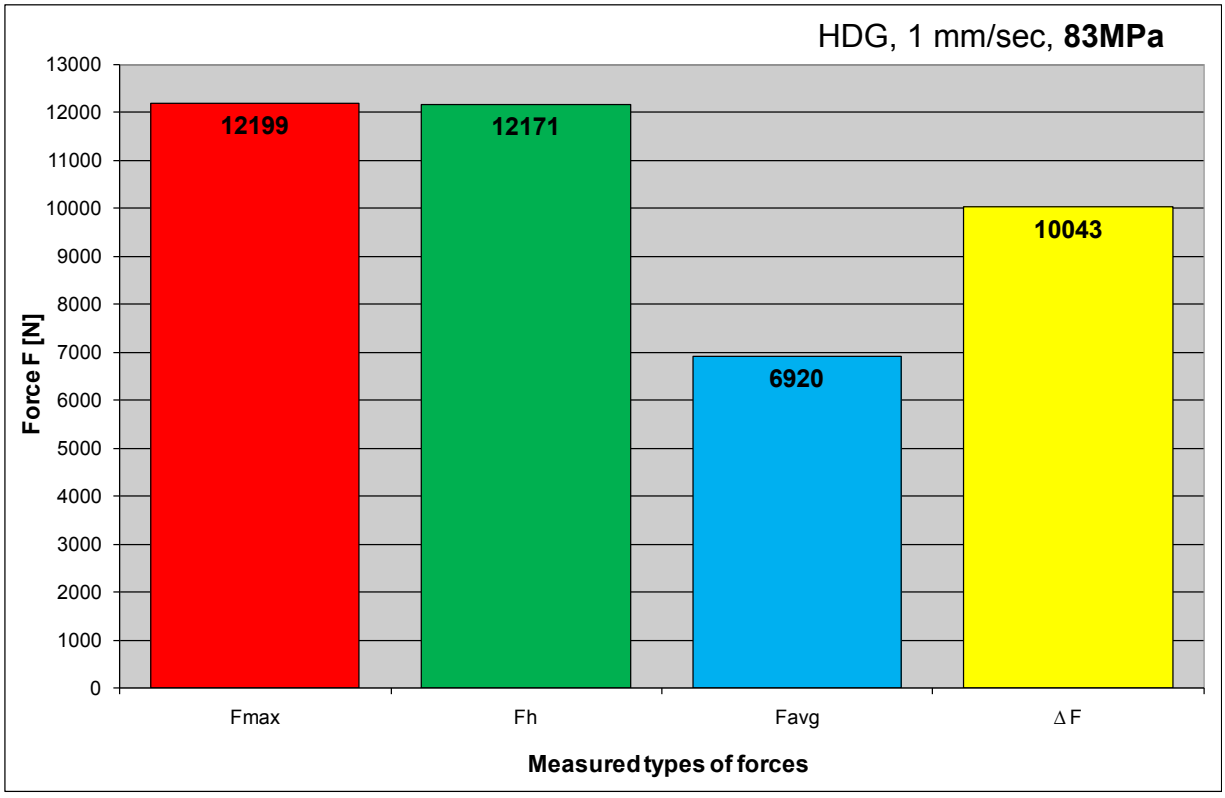

Fig. 5.13 *Measured forces for HDG, 1 mm/sec and 83 MPa*

Previous pages described results in light of forces. However, very often (and it was also needed in this thesis) there is necessary to describe tribological behavior just by one value – friction coefficient μ [1]. Equation (4) was used to compute friction coefficient arising from the strip drawing test. As a force, there was mostly taken F_h, in some cases F_{avg}– see Tab. 5.1. There is given an example of such computation for HDG, v = 1 mm/sec and p = 8 MPa. All magnitudes of friction coefficients vs. contact pressure are listed in Tab. 5.10 and graphically shown in Fig, 5.14.

$$\mu = \frac{F}{2.p.S} = \frac{1440}{2.8.400} = 0.225 \qquad [1] \qquad (4)$$

F	-	drawing force	[N]	(mostly F_h)
P	-	contact pressure	[MPa]	
S	-	contact area	[mm]	(S = 400 mm^2)

Tab. 5.10 *Measured friction coefficient for HDG, 1 mm/sec and all pressures*

Feed rate	Substrate	Feed rate	Contact Pressure
v= 1 mm/sec	**HDG**	**1 mm/sec**	**8÷83 MPa**

Friction coefficient μ [1]	**Contact pressure p [MPa]**					
	8	23	38	53	68	83
	0.225	**0.187**	**0.187**	**0.185**	**0.192**	**0.183**

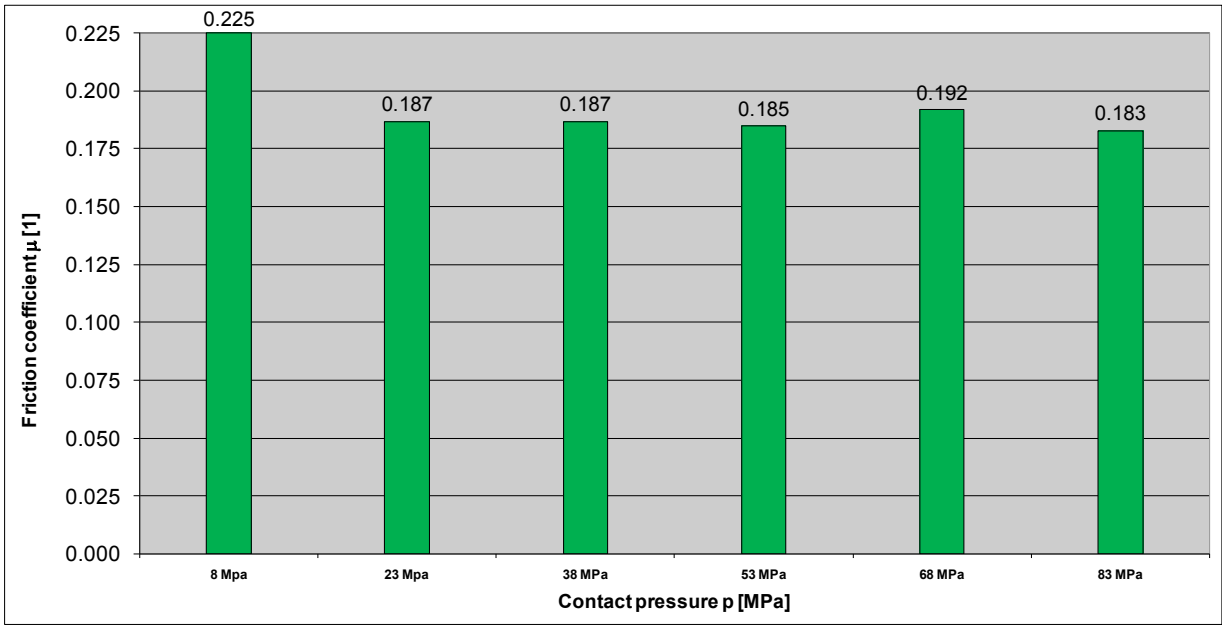

Fig. 5.14 *Friction coefficients for HDG, 1 mm/sec and all contact pressures*

5.4. Measured Results – HDG and All Used Feed Rates

In this chapter are summarized all results for HDG in dependence on all used feed rates. Fig. 5.15 and Fig. 5.16 show these results for 1 mm/sec and 10 mm/sec.

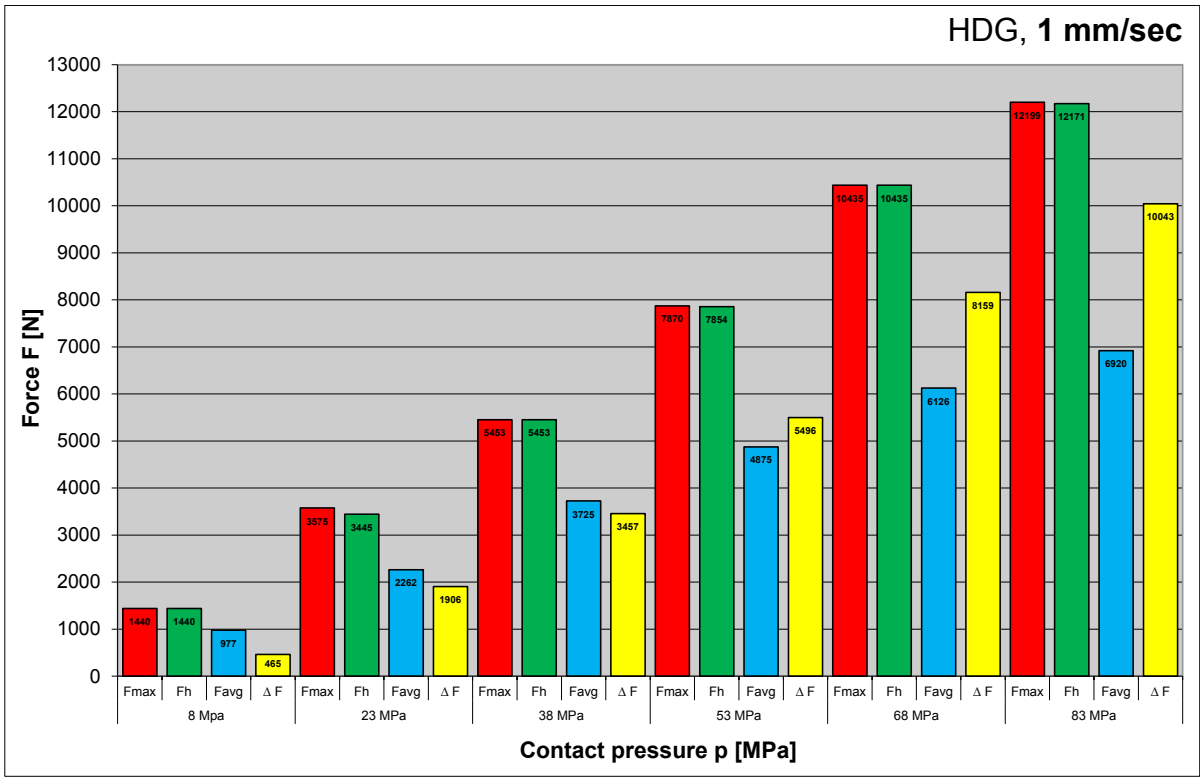

Fig. 5.15 *Measured forces for HDG, 1 mm/sec and all contact pressures*

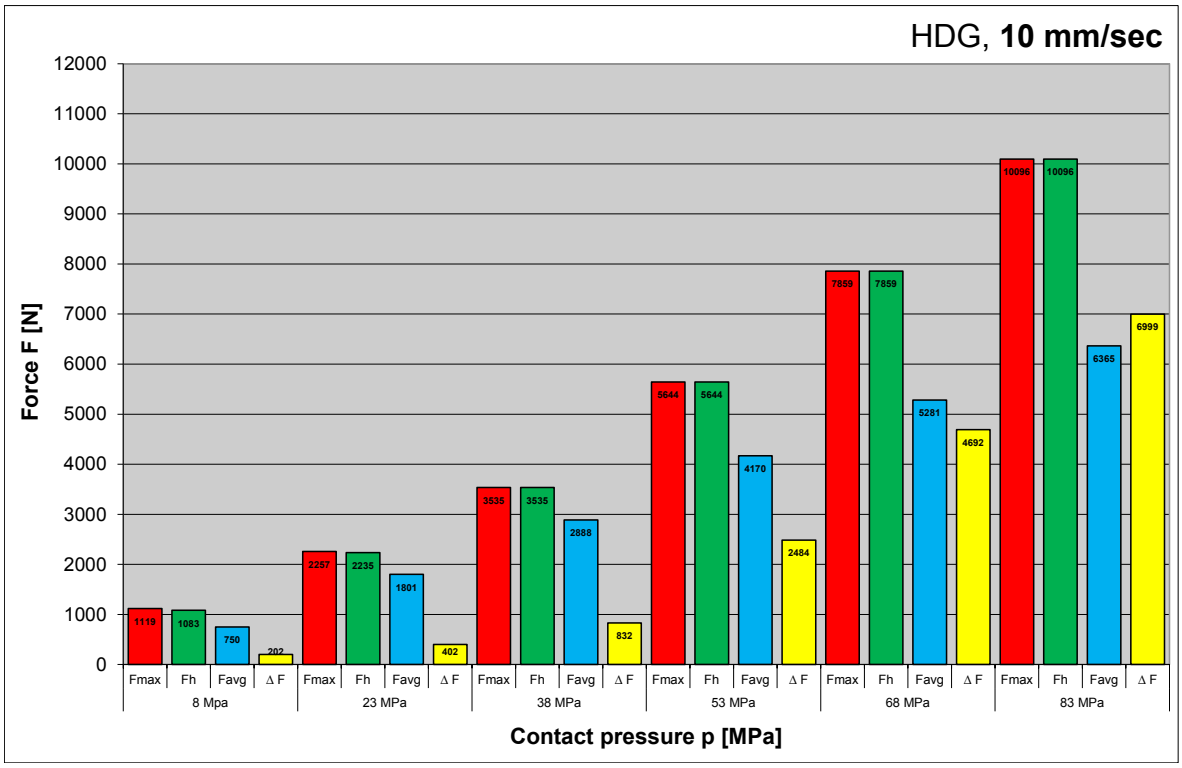

Fig. 5.16 *Measured forces for HDG, 10 mm/sec and all contact pressures*

In Fig. 5.17 and Fig. 5.18 are subsequently shown measured results for HDG and feed rate v = 50 mm/sec and v = 200 mm/sec, respectively.

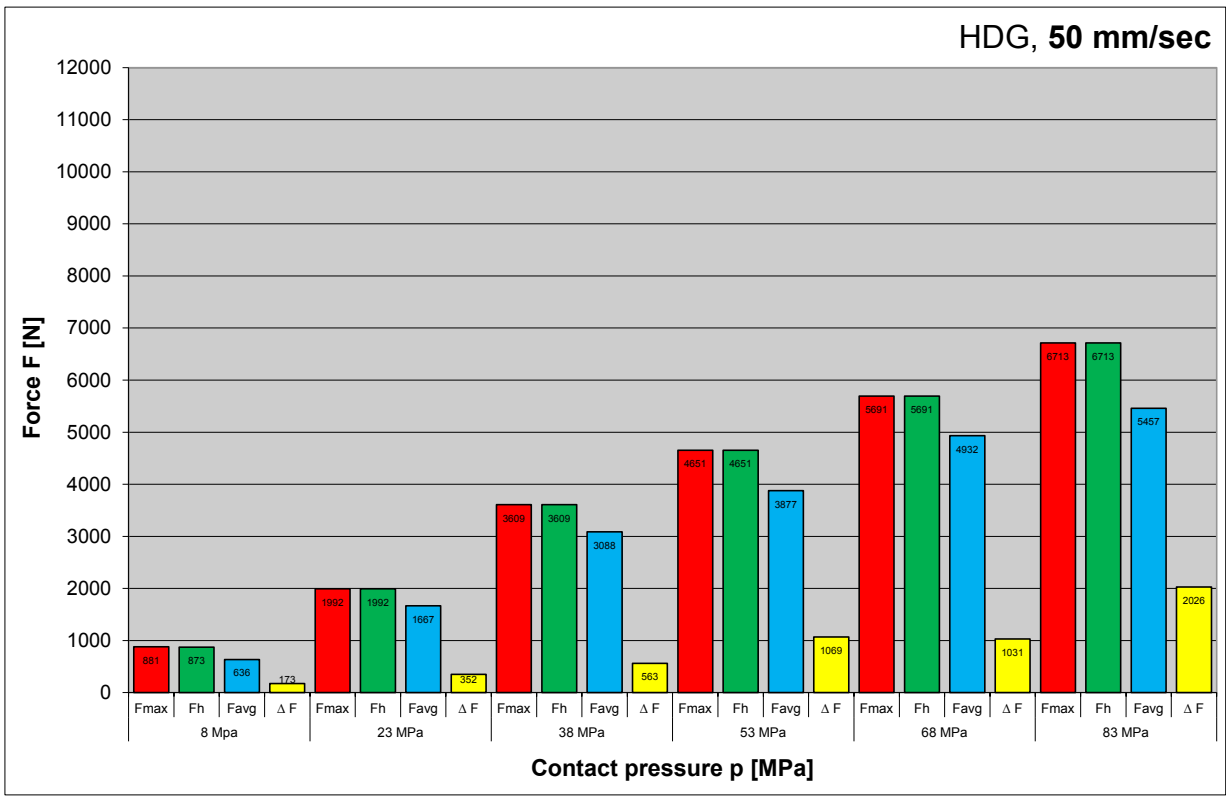

Fig. 5.17 *Measured forces for HDG, 50 mm/sec and all contact pressures*

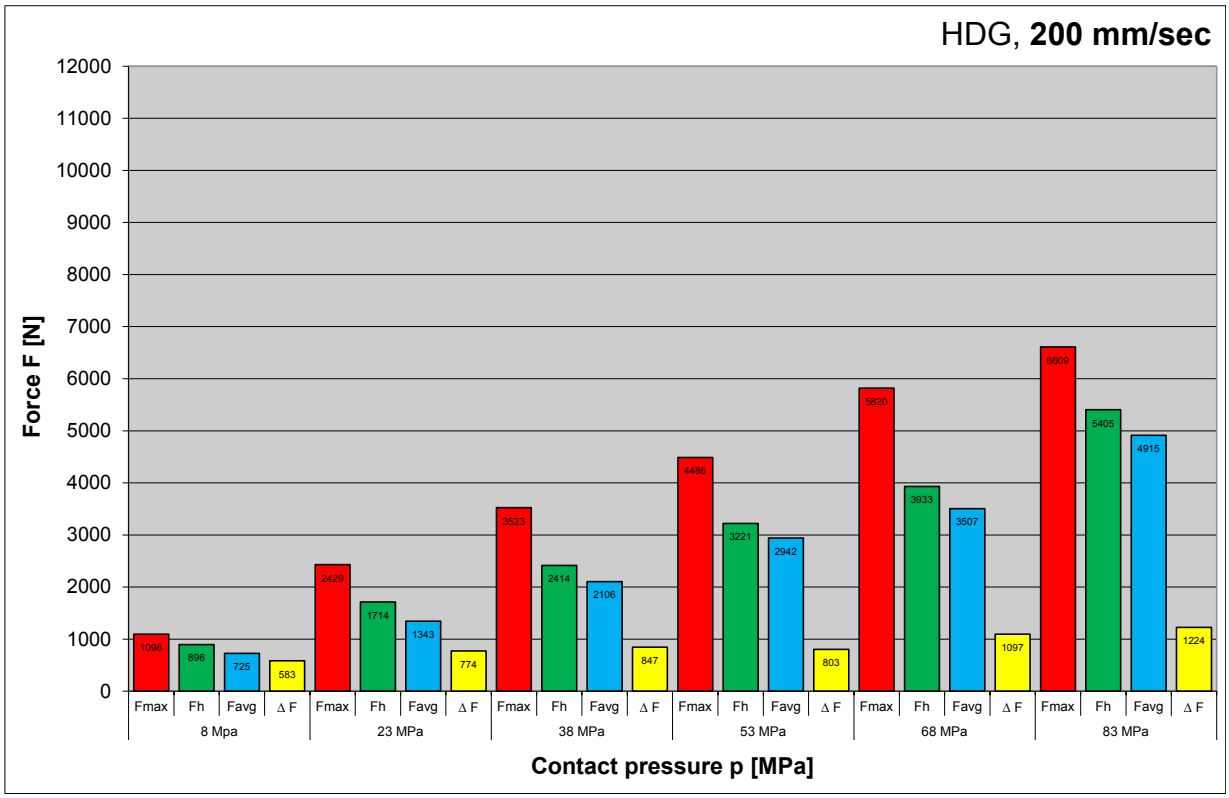

Fig. 5.18 *Measured forces for HDG, 200 mm/sec and all contact pressures*

In Fig. 5.19 are finally shown measured results for HDG and the maximal tested feed rate v = 400 mm/sec. Note that values of ΔF are much smaller than in the case of the minimal tested feed rate v = 1 mm/sec that was described in chap. 5.3.

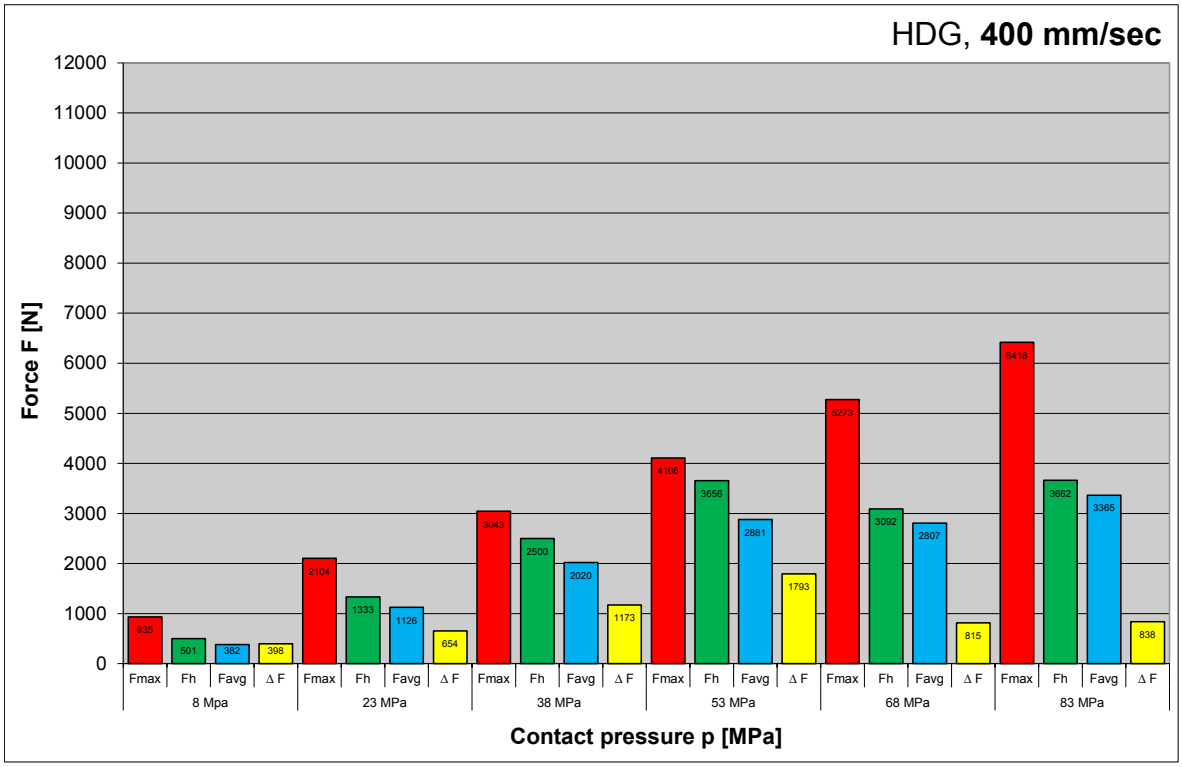

Fig. 5.19 *Measured forces for HDG, 400 mm/sec and all contact pressures*

In the graphs shown above are given the major results of the evaluated forces (except F_{min}) for HDG in dependence on contact pressure p [MPa] for every used feed rate v [mm/sec].The 1st graph (Fig. 5.15) has been already described in the previous chapter. There is possible to observe tendency that is typical of tribological measurement: the higher feed rate, the lower forces (thus also friction coefficient).On the other hand, the higher contact pressure doesn´t always mean also increase of the friction coefficient (see Fig. 5.25). Quite interesting result arouse from the comparison between v = 10 mm/sec and v = 50 mm/sec (Fig. 5.16 and Fig. 5.17) in light of peak-to-valley force ΔF for 83 MPa (6999 N and 2026 N). Such decrease of its magnitude means that there was not stick-slip effect (galling) under 50 mm/sec. From the overall results point of view, it can be seen that measured forces for feed rate 10 mm/sec are only 80% of 1 mm/sec that is taken as 100%. Keeping the same basic (1 mm/sec), the subsequent measured feed rates had forces as following: for feed rate 50 mm/sec wereforces60%, for feed rate 200 mm/sec were these values 50% and for feed rate 400 mm/sec were only 40% of forces for 1 mm/sec.

5.5. Measured Results – NIT and All Used Feed Rates

In this chapter are summarized all results for NIT in dependence on all used feed rates. Fig. 5.20 and Fig. 5.21 show these results for 1 mm/sec and 10 mm/sec.

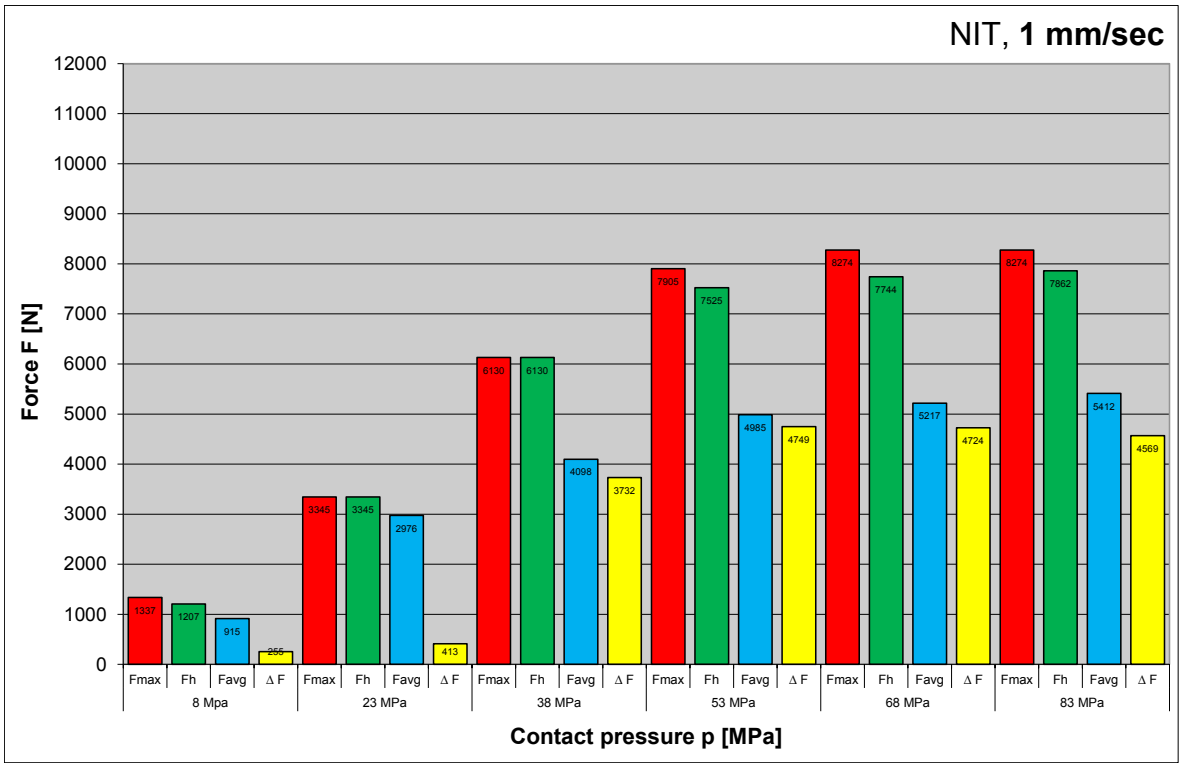

Fig. 5.20 *Measured forces for NIT, 1 mm/sec and all contact pressures*

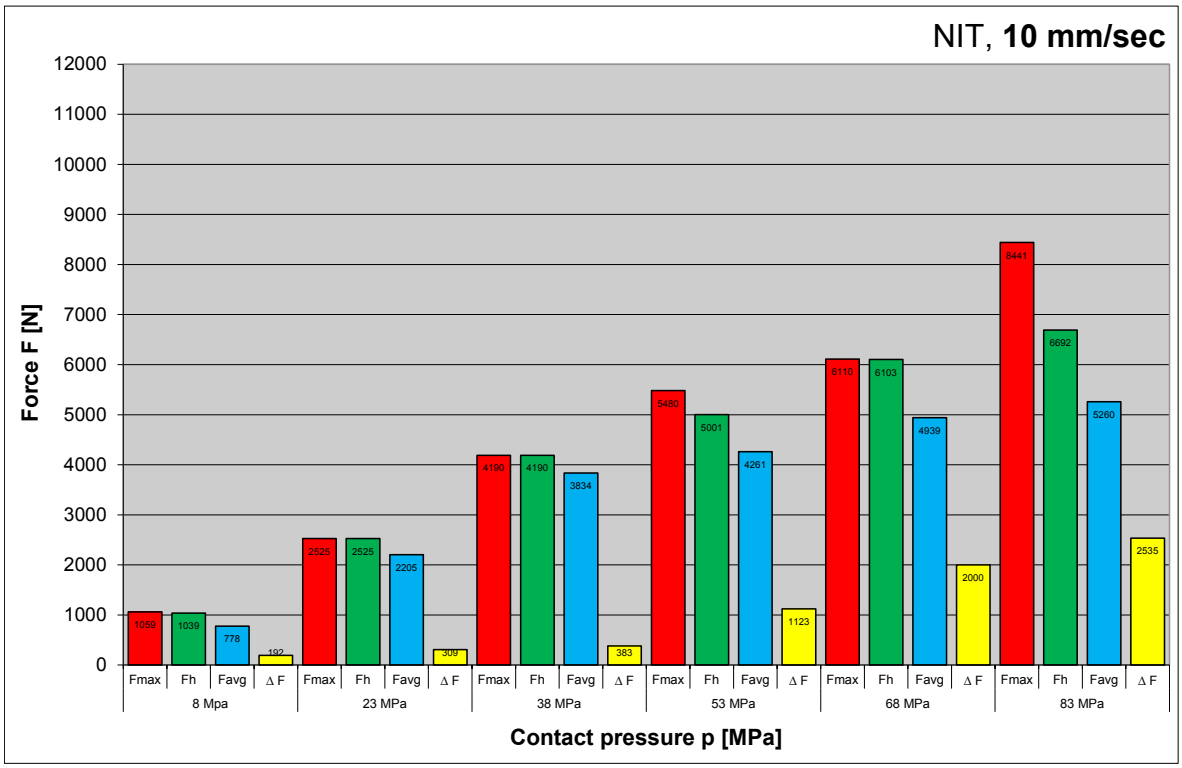

Fig. 5.21 *Measured forces for NIT, 10 mm/sec and all contact pressures*

In Fig. 5.22 and Fig. 5.23 are subsequently shown measured results for NIT and feed rate v = 50 mm/sec and v = 200 mm/sec, respectively.

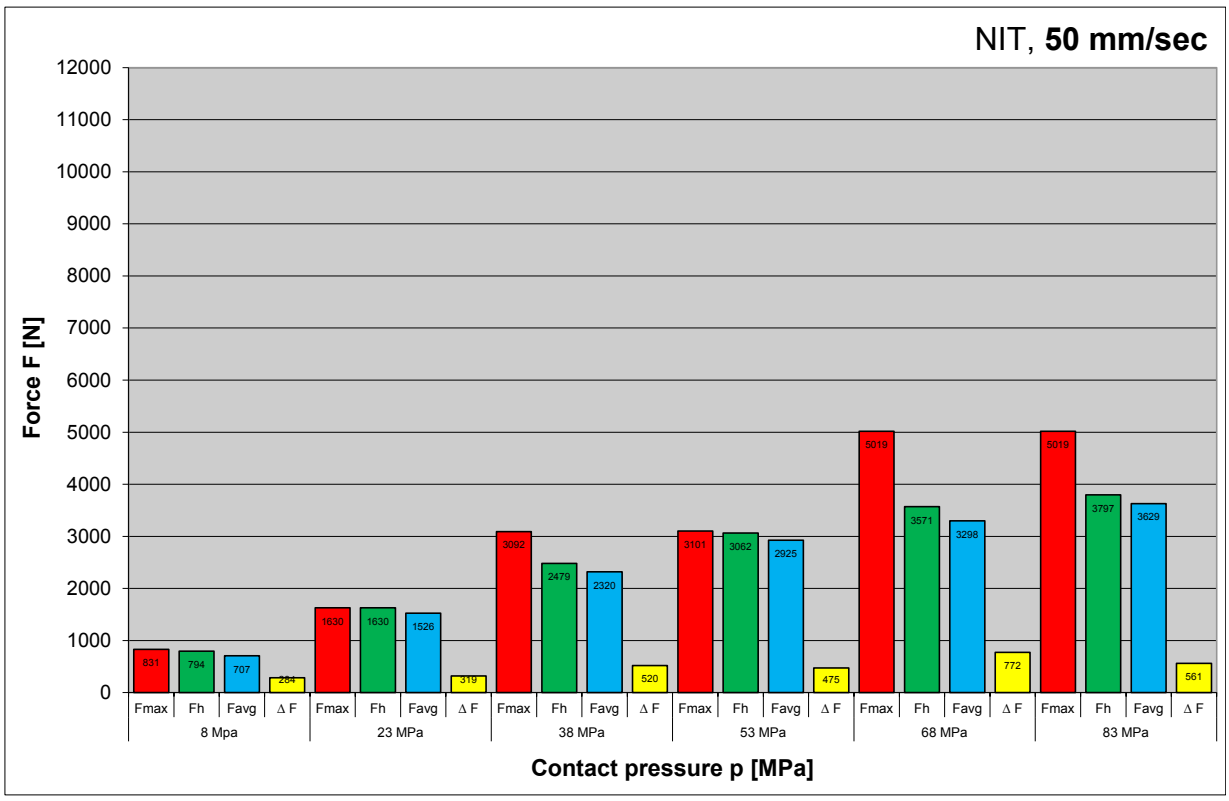

Fig. 5.22 *Measured forces for NIT, 50 mm/sec and all contact pressures*

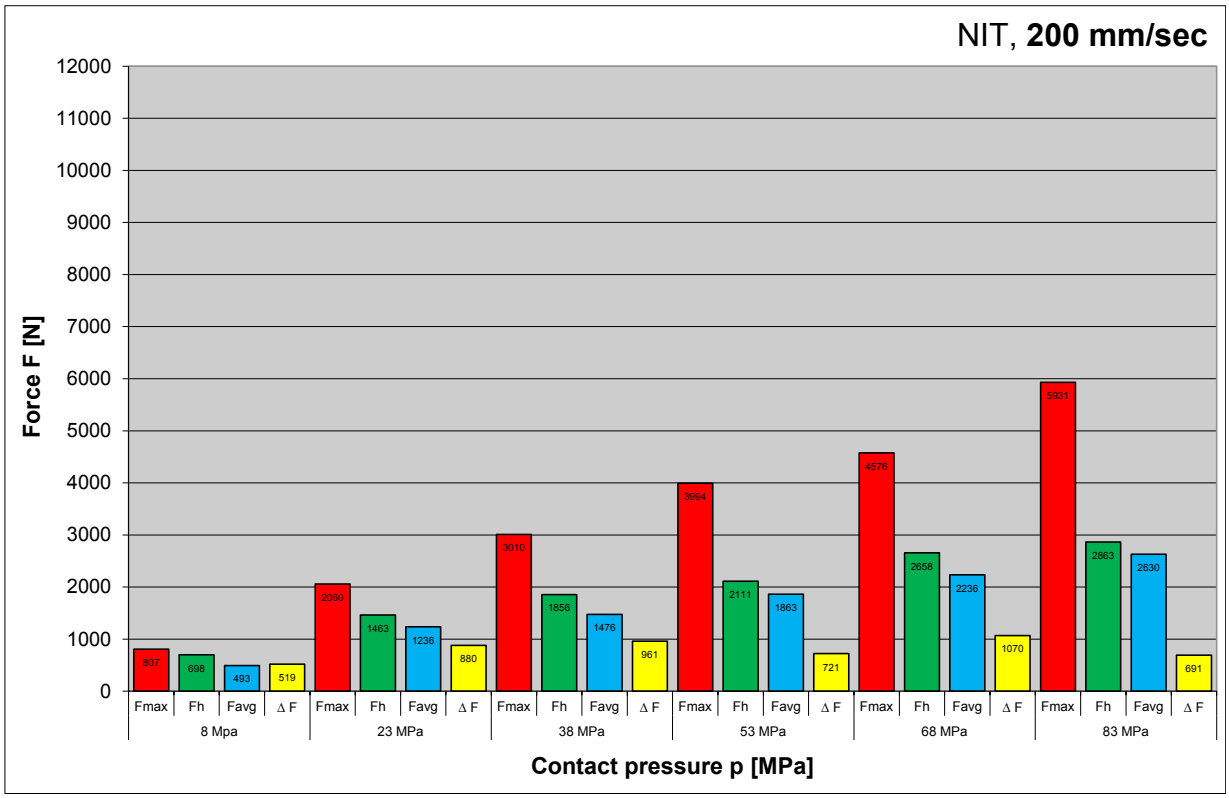

Fig. 5.23 *Measured forces for NIT, 200 mm/sec and all contact pressures*

In Fig. 5.24 are finally shown measured results for NIT and the maximal tested feed rate v = 400 mm/sec. Note again the basic influence of feed rate on the final magnitudes of forces compared to minimal feed rate v = 1 mm/sec (see Fig. 5.20).

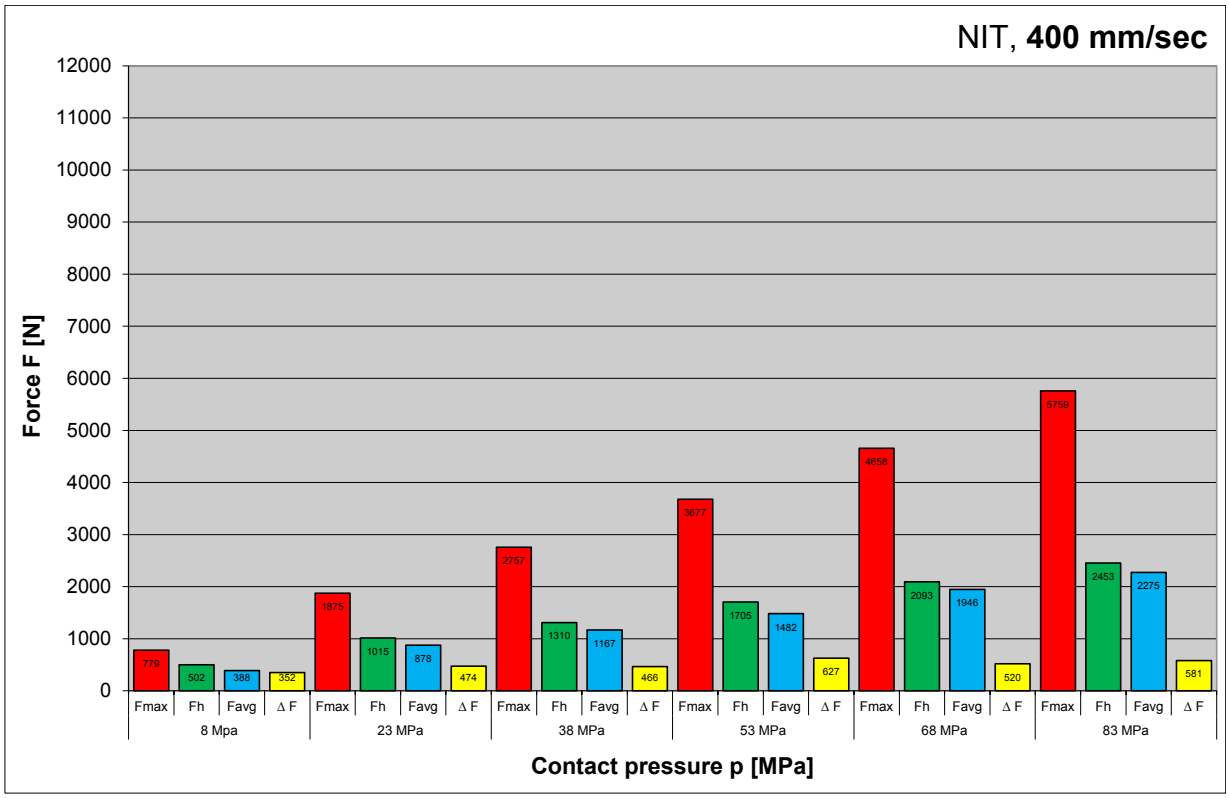

Fig. 5.24 *Measured forces for NIT, 400 mm/sec and all contact pressures*

In the graphs shown above are given the major results of the evaluated forces (except F_{min}) for NIT in dependence on contact pressure p [MPa] for every used feed rate v [mm/sec]. Already from the 1st graph (Fig. 5.20) it is possible to observe lower magnitudes of evaluated forces – especially under high contact pressures (as it is said to be from the producer). Generally, there are the same tendencies as before. In this case, other quite interesting result arouse from the comparison of peak-to-valley force ΔF for v = 1 mm/sec, because stick-slip effect took place not until contact pressure 38 MPa (23 MPa for HDG samples). Moreover, it can be seen that F_{max} isn´t mostly equal to F_h from 10 mm/sec, which means the more stable process compared to HDG substrates (there it was from 50 mm/sec). From the overall results point of view, it can be seen that forces for feed rate 10 mm/sec are approx. 90% of 1 mm/sec (taken as 100%). Keeping the same basic (1 mm/sec), the subsequent measured feed rates had forces as following: for feed rate 50 mm/sec are forces 60%, for feed rate 200 mm/sec are these values 50% and for feed rate 400 mm/sec are only 40% of forces for 1 mm/sec.

Also in the case of substrate NIT was as an output to evaluate its tribological behavior used friction coefficient μ [1] instead of forces. Again, equation (4) was used to compute friction coefficient arising from the strip drawing test. As a force, there was mostly taken $F_{h,}$ in some cases F_{avg} – see Tab. 5.1. There is also given an example of such computation for NIT, v = 1 mm/sec and p = 8 MPa. All magnitudes of friction coefficients vs. contact pressure are listed in Tab. 5.11 and graphically shown in Fig, 5.25. Note that values under the high contact pressure are decreasing.

$$\mu = \frac{F}{2.p.S} = \frac{1207}{2.8.400} = 0.189 \qquad [1] \qquad (4)$$

F	-	drawing force	[N]	(mostly F_h)
P	-	contact pressure	[MPa]	
S	-	contact area	[mm]	(S = 400 mm^2)

Tab. 5.11 *Measured friction coefficient for NIT, 1 mm/sec and all pressures*

Feed rate	Substrate	Feed rate	Contact Pressure
v = 1 mm/sec	**NIT**	**1 mm/sec**	**8÷83 MPa**

Friction coefficient μ [1]	**Contact pressure p [MPa]**					
	8	23	38	53	68	83
	0.189	**0.182**	**0.202**	**0.177**	**0.142**	**0.118**

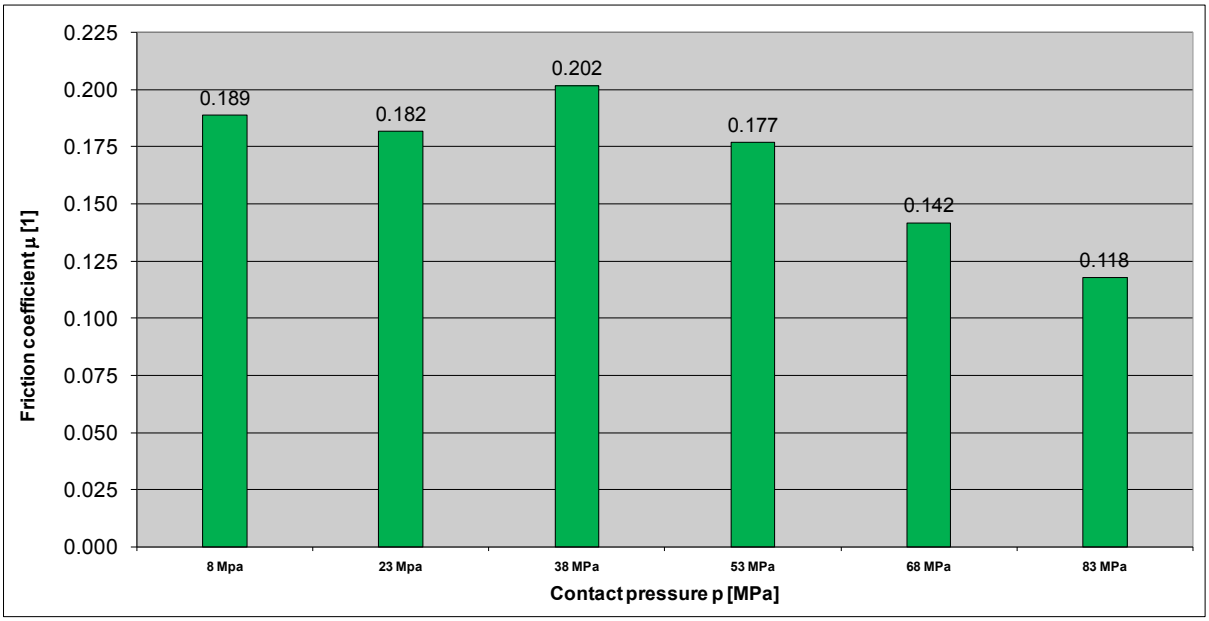

Fig. 5.25 *Friction coefficients for NIT, 1 mm/sec and all contact pressures*

5.6. 3D Color Maps Surface Graphs for HDG and NIT

There were quite a lot of data to be compared (see previous chapters) and thus there was necessary to shown them in the simple way. That is why there were finally used 3D color map surface graphs because they offer a very easy way how to compare the measured results and to find out the difference between them. In this chapter is described method how to create them and also evaluation of results.

Empty 3D graph is shown in Fig. 5.26 under the following conditions: feed rate on X-axis, contact pressure on Y-axis and friction coefficient on Z-axis. Then (see Fig. 5.27), the used intersections of feed rates (1, 10, 50, 200 and 400 mm/sec) on X-axis and contact pressures (8, 23, 38, 53, 68, 83 MPa) on Y-axis are shown as small black dots. Finally, the 3D scatter graph using also magnitudes of relevant friction coefficient on Z-axis is shown in Fig. 5.28. In this case, these friction coefficient values are drawn from the points arising from the intersections of X-axis and Y-axis (used testing parameters in light of feed rate and contact pressure). However, by using such 3D scatter graph, it is difficult to compare results measured from tested substrates HDG and NIT. That is why there were subsequently used 3D color map surface graphs (see Fig. 5.30 and 5.31) to compare final results.

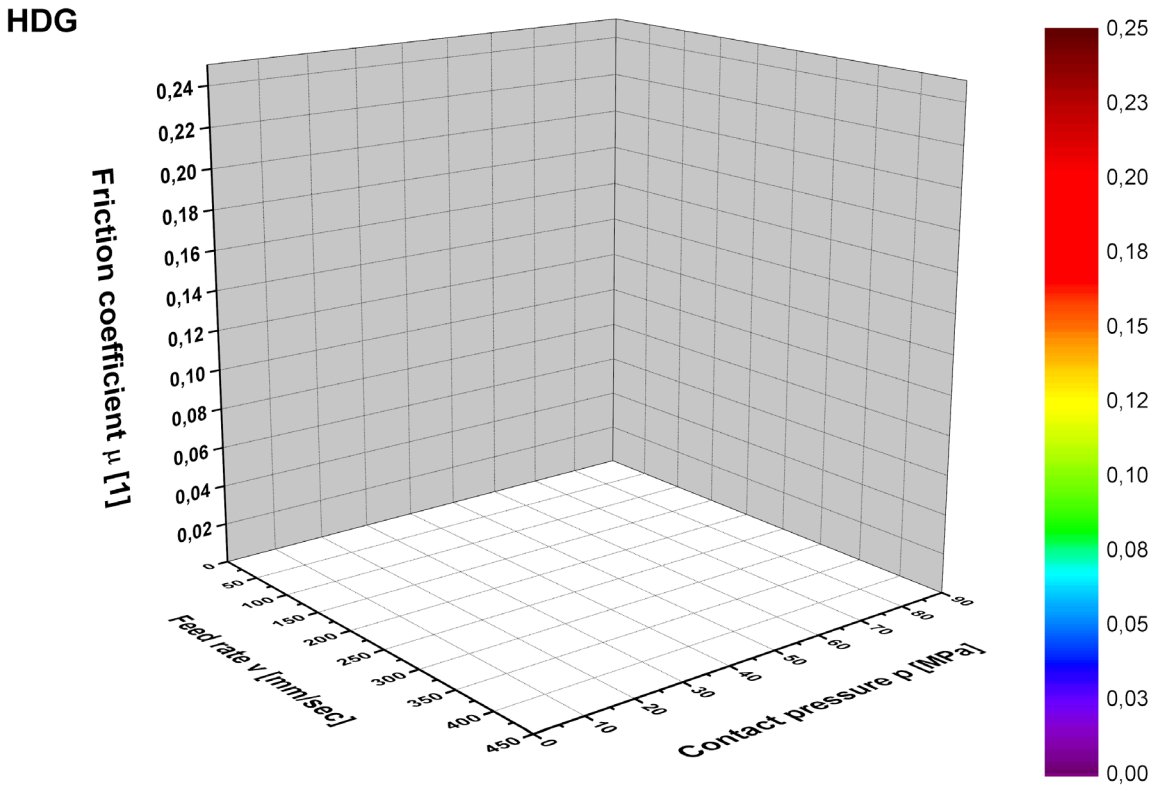

Fig. 5.26 *Empty 3D graph under relevant conditions*

On this page, the point graph (Fig. 5.27) arising from testing parameters (small dots on X-Y plane) and scatter graph (Fig. 5.28) arising from final result are shown

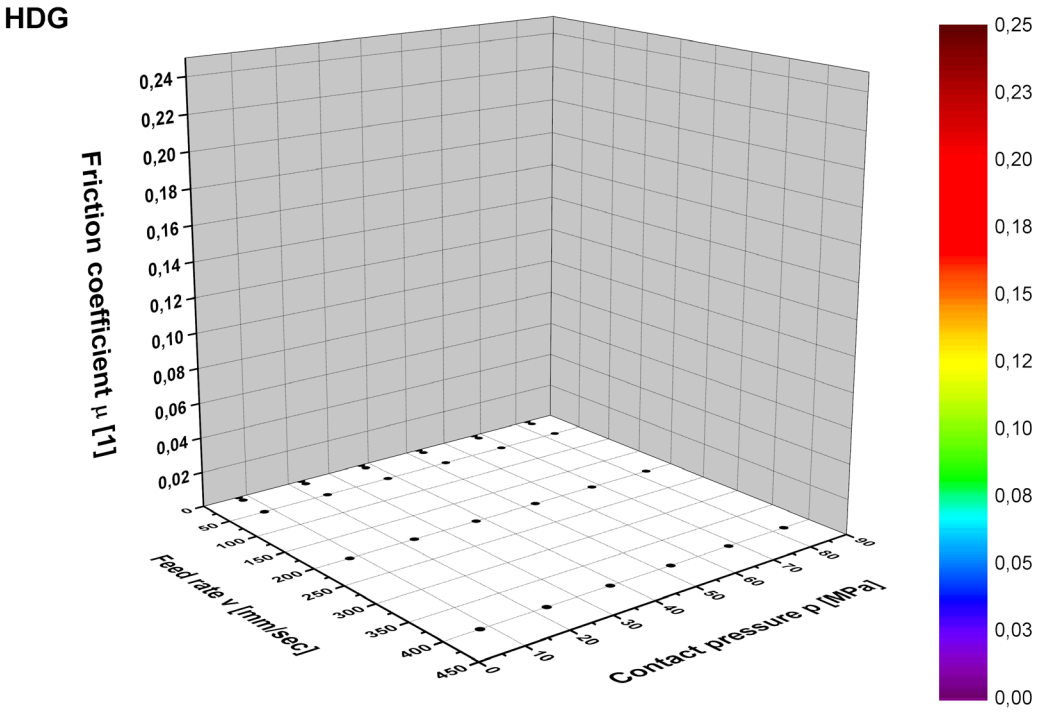

Fig. 5.27 *3D graph with points arising from testing parameters (X-Y plane)*

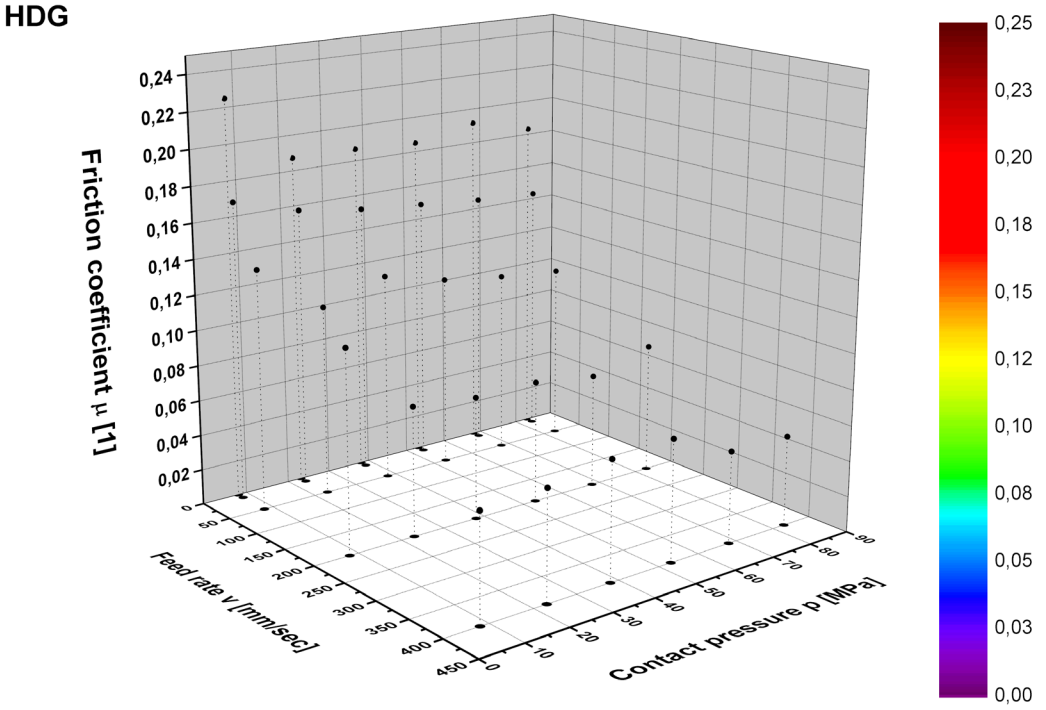

Fig. 5.28 *3D scatter graph arising from results of HDG*

On this page is described how the 3D color map surface graphs were created by the software OriginPro 9.0. Firstly, there was necessary to perform so-called XYZ gridding from measured results. On the left side of Fig. 5.29 can be seen X-Y-Z columns which consist of the feed rate v (X-column), contact pressure p (Y-column) and friction coefficient μ (Z-column). Then, Z-column (consisting of friction coefficient values) was selected and its values were converted by the matrix conversion method called as XYZ gridding into 25x25 matrix- as it is shown below. Series of 25x25 nodes can be seen on the 3D color map surface graph. To create such required nodes on the 3D color map surface, a final matrix of 25x25 was created by the method called as Thin Plate Spline. This matrix with 25 columns and 25 rows is shown in the right bottom of Fig. 5.29.

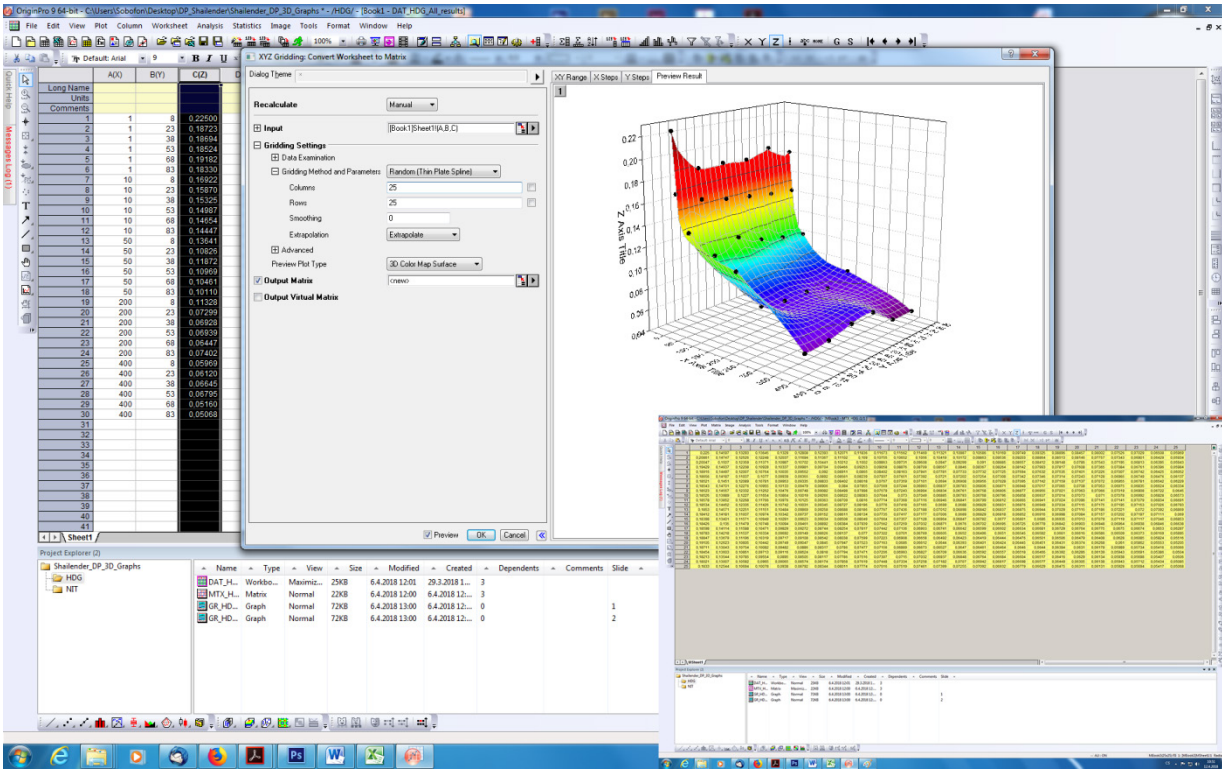

Fig. 5.29 *Creation of 3D color map surface graph by using matrix 25x25*

There are a lot of gridding methods, but a gridding method called as thin plate spline was used in this evaluation. After converting the friction coefficient values into 25x25 matrix by this method, the own 3D color map surface was created. Such procedure was used both for HDG and NIT substrate. The own gridding points are also shown in these graphs as grey color surface lines together with the own results of friction coefficient values for the relevant testing parameters (big black dots), which were already used before in the 3D scatter graphs (Fig. 5.28).

Below, the final 3D color map surface graphs both for HDG (Fig. 5.30) and NIT (Fig. 5.31) are shown – in both of them are used gridding lines and scatter points.

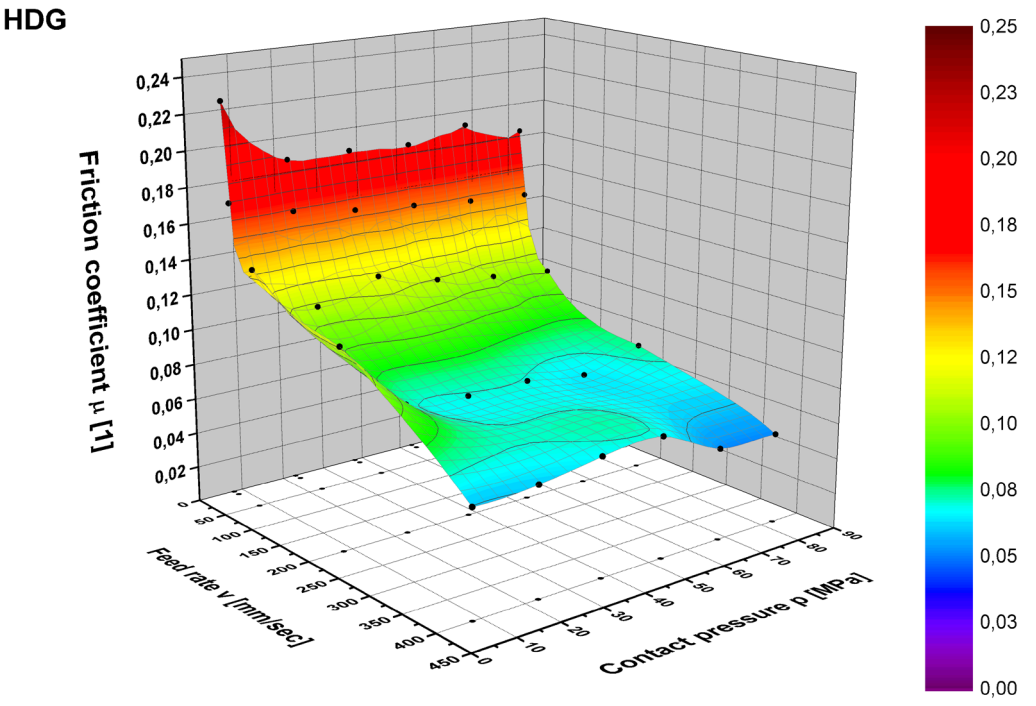

Fig. 5.30 *3D color map surface graph for* ***HDG***

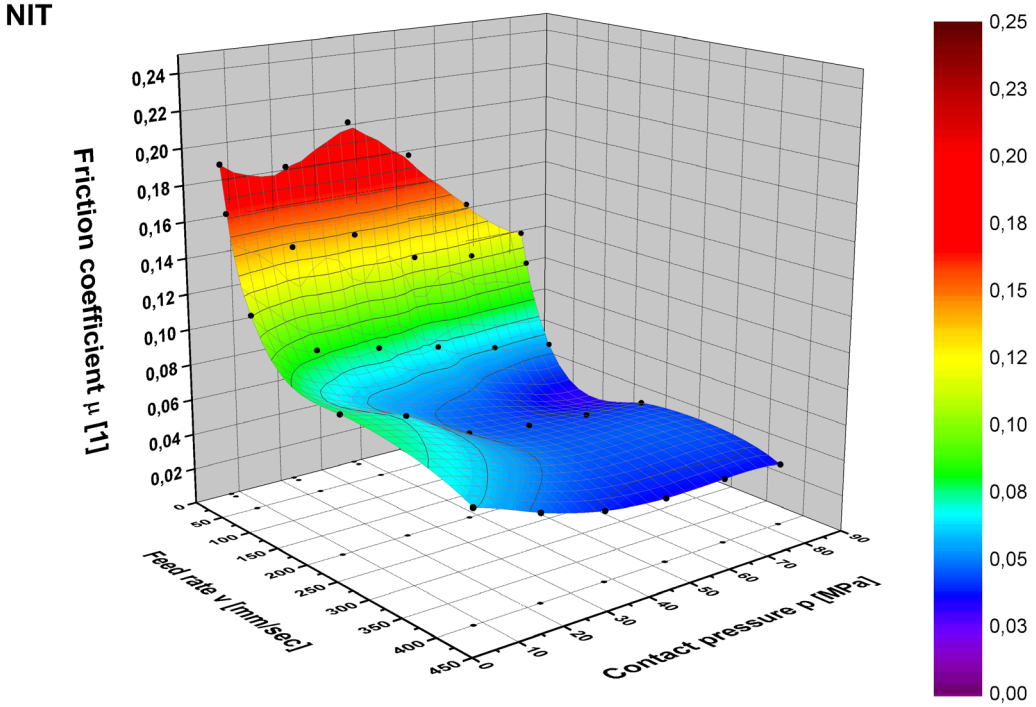

Fig. 5.31 *3D color map surface graph for* ***NIT***

5.7. Results Discussion and Recommendations

In this strip drawing test, samples with substrate of HDG and NIT were tested under the tribological conditions as following: feed rates v [mm/sec] of 1, 10, 50, 200 and 400 mm/sec and contact pressures p [MPa] of 8, 23, 38, 53, 68 and 83 MPa. After the testing, the forces as F_{max}, F_h, F_{avg}, F_{min} and ΔF were obtained from every combination of feed rate and contact pressure. These measured forces were used for the computation of friction coefficient μ [1]. After that, these friction coefficient values were converted into 25x25 matrix and 3D color map surface graphs were created with the help of such matrix to enable better overview of results.

The comparison by the side views on 3D color map surfaces (showing results both for HDG and NIT) can be seen in Fig. 5.32. The differences in results can be compared by the surface color and relevant color on the scale to the right. In both cases, as feed rate v [mm/sec] and contact pressure p [MPa] increases, the friction coefficient μ [1] decreases. However, in general comparison, results of NIT are better than HDG, because almost the whole surface is beneath the HDG one. As it was discussed before, under the low feed rates and low contact pressures, the friction coefficients for HDG and NIT are almost the same. On the other hand, under the high feed rates and high contact pressures, NIT is much better than HDG. Under the low contact pressures and high feed rates, the results are very similar. Finally, under the low feed rates and high contact pressures, NIT is better than HDG.

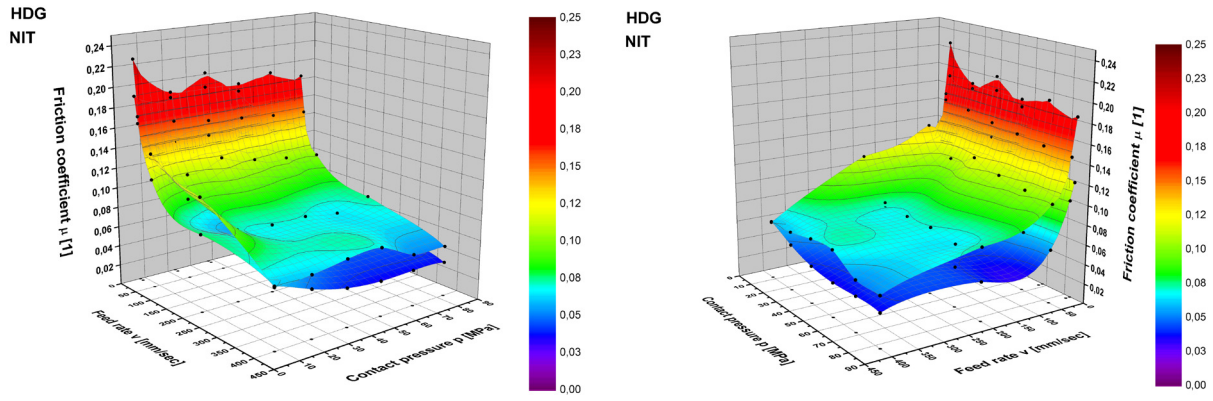

Fig. 5.32 *Side views of results (HDG is the upper surface and NIT is the lower one)*

To make overview of these results a little bit better, perpendicular views on the 3D color map surfaces is shown in Fig. 5.33 – HDG (left) and NIT (right). By the comparison of the results shown in this approach (perpendicular view), it can be

again seen that under the low feed rates and high contact pressures, the friction coefficient of HDG is higher than NIT. Under the high feed rates and high contact pressure, the friction coefficient of HDG is much higher than NIT. And finally again, under the low feed rates and low contact pressures, results are almost the same.

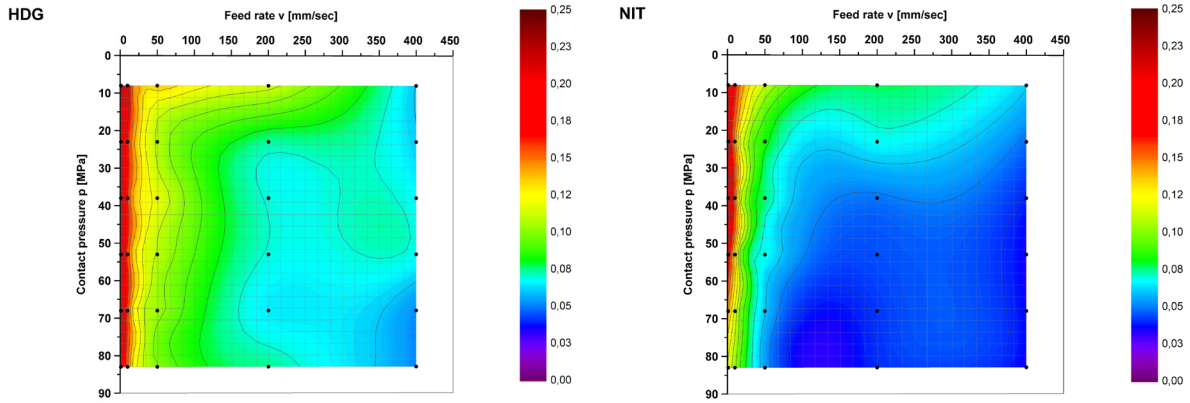

Fig. 5.33 *Perpendicular view of results: HDG (left) and NIT (right)*

However, for better comparison and description of results in light of math, there was calculated the volume beneath the matrix surfaces from zero panel by using the software OriginPro 9.0. The software applied double integration in two directions (axis X-Y) to sum every point under the matrix surface. So in this case, volume was computed by using two different quantities - feed rate and contact pressures. The volumes beneath the matrix surface for HDG and NIT are listed in Tab. 5.12.

Tab. 5.12 *Volume beneath the 3D surface of HDG and NIT*

Volume beneath surface [MPa·mm·sec^{-1}]	**Substrate**	
	HDG [MPa·mm·sec^{-1}]	**NIT** [MPa·mm·sec^{-1}]
	2514.1	**1748.3**

The software computed the volume under the matrix surface to have a rapid comparison of the results both for HDG and NIT only as two values. Here again was proved that NIT is better than HDG. Nevertheless, just by having this one value there cannot be described the tribological behavior of HDG and NIT. Generally, tribological behavior can be properly described only by 3D color map surface.

Finally, in this experiment was proved that NIT surface treatment is better than HDG one in light of tribology (especially under the high feed rates and high contact pressures). But there was not discussed the price for the production of these surfaces, the purchase price for tools, resistance to corrosion and so on.

6. CONCLUSION

This diploma thesis was about the influence of different surface coatings on the magnitude of friction coefficient. As testing samples there were used Hot Dip Galvanized (HDG) and New Inorganic Treatment (NIT)coatings on deep drawing steel sheets. These surfaces were subjected to the tribological test termed as strip drawing test under different conditions of feed rates and contact pressures. For evaluation and comparison of results from both tested surface coatings, there were used both common 2D bar graphs and 3D color map surface graphs of friction coefficient for better evaluation in light of one value as well as the whole surface.

In the theoretical part of this thesis was described the tribology itself including different types of surfaces, roughness parameters and tribological tests. Moreover, there were also described materials that are commonly used at car-body design as e.g. deep-drawing steels, ultra high-strength steels or composites. Finally, some surface treatments (to be specific CVD, PVD, EG and HDG) were described as well.

In the experimental part of this thesis was primarily performed strip drawing test for two different types of surface coatings (HDG and NIT). At the beginning, samples were cut onto required dimensions, degreased and lubricated before the test. The test was done under the following tribological parameters: feed rate 1, 10, 50, 200, 400 mm/sec and contact pressure 8, 23, 38, 53, 68, 83 MPa. After the test, results as measured forces and friction coefficients in dependence on contact pressure were tabulated and shown by 2D bar graphs. For better description and analysis of results, 3D color map surface graphs were prepared as well. From the basic comparison arising of these 3D surfaces, NIT revealed a better results especially under the higher feed rates and contact pressures (the friction surface is there situated much lower than HDG one). On the other hand, under the low feed rate and low contact pressures, results were almost the same. Just to compare these results from one value, volumes beneath the surfaces were computed and NIT was about 30% lower. Thus finally it can be stated that NIT revealed better tribological behavior under high feed rates and high contact pressures, as it was expected. On the other hand, in this thesis was not evaluated e.g. economical aspect of using NIT surfaces. Moreover, this was just a first testing and more tests under different conditions (other feed rates, types of lubricants, also different surface coatings and so on) are needed to be performed to verify such basic conclusion.

References

[1] Fraunhofer [online]. 2017 [qut. 2017-08]. Available from: https://www.ifam.fraunhofer.de/en/Profile/Locations/Bremen/Adhesive_Bonding_Surfaces/Plasma_Technology_Surfaces/Tribology.html

[2] STACHOWIAK, G.W., BATCHELOR, A.W. *Engineering tribology.* 4th ed. Oxford: Butterworth - Heinemann, 2014. p. 884. ISBN 978-0-123-9-70473.

[3] Stle [online] . 2017 [qut.2017-08]. Available from: http://www.stle.org/files/TLTArchives/2016/06_June/Webinars.aspx

[4] TOTTEN, G.E. ed. *Handbook of Lubrication and Tribology: Volume I – Application and Maintenance.* 2nd ed. Boca Raton: CRC Press, 2006, p. 1159. ISBN 978-0-8493-2095-8.

[5] University of Delaware[online]. 2017 [qut. 2017-08].Available from: https://www.rewitec.com/assets/images/9/Tribometre_Vinci_1-c8e8dc49.jpg

[6] Leonardo da Vinci [online]. 2017 [qut. 2017-08]. Available from: https://www.leonardodavinci.net/

[7] BOOSER, E.R. *CRC handbook of lubrication and tribology (Volume II - Theory & Design).* Revised Edition, 1983. p. 3-31. ISBN 0-8493- 3902- 2 (v.2).

[8] LUDEMA K.C, *Friction, wear, lubrication.* CRC press, 1996. p. 86. ISBN 0-8493-2685-0.

[9] Brake system [online]. 2017 [qut. 2017-08]. Available from: http://cdn.bmwblog.com/wp-content/uploads/bmw-m3-m4-brakes.jpg

[10] Cartoq [online]. 2017 [qut. 2017-08]. Available from: http://www.cartoq.com/when-to-replace-your-clutch-plates-warning-signs/

[11] MANG, T., DRESEL, W. Lubricants and Lubrication. 2nd ed. Weinheim: WILEY- VCH Verlag, 2007. p. 894. ISBN: 978-3-527-31497-3.

[12] KHUN, H.,MEDLIN, D., ed. ASM HANDBOOK Volume 8 – *Mechanical testing and Evaluation. 10th ed.* Materials Park: ASM International, 2000. p. 998. ISBN 0-87170-389-0.

[13] Moulding and casting [online]. 2017 [qut. 2017-09]. Available from: http://www.wizardsdenspfx.com/casting.htm

[14] Picquery [online]. 2017 [qut.2017-09]. Available from:http://www.substech.com/dokuwiki/lib/exe/fetch.php?w=&h=&cache=cache&media=lubrication_regimes.png

[15] MING QUI, S.L. ed. *Bearing tribology.* Berlin-Heidelberg: Springer Verlag, 2017. p. 325 ISBN 978-3-662-53097-9.

[16] Machinery lubrication [online]. 2017 [qut. 2017-09]. Available from: http://www.machinerylubrication.com/Read/30741/lubrication-regimes

[17] SEMIATIN, S. L. ed. *ASM HANDBOOK Volume 14 –Forming and Forging. 6th ed.* Materials Park: ASM International, 2004. p. 978. ISBN 0-87170-020-4.

[18] SEMIATIN, S. L. ed. *ASM HANDBOOK Volume 14B – Metalworking: Sheet Forming. 2nd ed.* Materials Park: ASM International, 2006. p. 978. ISBN 0-87170-710-1.

[19] DAVIES, G. *Materials for automobile bodies.*1st ed., Oxford: Butterworth-Heinemann Publications, 2012. p. 285. ISBN 978-0-08-096979-4.

[20] ASHBY, M.F. *Materials Selection in Mechanical Design*. 3rded. Oxford: Butterworth-Heinemann, 2005. p. 603. ISBN 0-7506-6168-2.

[21] DAVIES, G*. Materials for Automobile Bodies.* OXFORD: Butterworth-Heinmann, 2003. p. 277. ISBN 0-7506-5692-1.

[22] Steels [online]. 2017 [qut. 2017-09]. Available from: https://sc01.alicdn.com/kf/HTB1isdJSpXXXXXNaFXXq6xXFXXX5/Baosteel-Bhg960-China-Ultra-High-Strength-Steel.jpg

[23] Vision on polymers [online]. 2017 [qut. 2017-09]. Available from: https://vip-fo.de/products/standard-thermoplastics/?lang=en

[24] IDI Composites [online].2017 [qut. 2017-09]. Available from: http://www.idicomposites.com/markets-stc.php

[25] Carbon composites [online].2017 [qut.2017-09]. Available from: http://carboncompositesinc.com/

[26] HOLMBERG, K. and MATHEWS*, A. Coatings tribology. 2nded*. Oxford: Elsevier, 2009. p. 175. ISBN 978-0-444-52750-9.

[27] Henkel [online]. 2017 [qut. 2017-09]. Available from: http://www.henkel-adhesives.com/automotive/surface-treatment-39739.htm

[28] TRACTON, A.A. *Coating materials and surface coatings.* London: Taylor & Francis Group, 2007. p. 464. ISBN 1-4200-4404-4.

[29] *Chemistry of Electronic Materials* [online].2017 [qut. 2017-09]. Available from: http://archive.cnx.org/contents/9bbbe39c-a840-4461-882ce31f8a0125e6@2/chemical-vapor-deposition

[30] Merck [online]. 2017 [qut. 2017-09]. Available from: http://www.sigmaaldrich.com/materials-science/material-science-products.html?TablePage=108832720

[31] Chemistry 58 [online].2017 [qut. 2017-09]. Available from: https://chemistry58.wikispaces.com/Electroplating

[32] AGA [online]. 2017 [qut. 2017-09]. Available from: https://www.galvanizeit.org/hot-dip-galvanizing/what-is-hot-dip-galvanizing-hdg/hdg-process